Electromagnetic Scattering Parameters of Subshields, Electromagnetics, 1986 pp. 47-59

INTERACTION NOTES

NOTE 427

APRIL 1983

USE OF MATRIX NORMS OF INTERACTION SUPERMATRIX BLOCKS FOR SPECIFYING ELECTROMAGNETIC PERFORMANCE OF SUBSHIELDS

F.C. Yang

Dikewood
Division of Kaman Sciences Corporation
1613 University Blvd., NE
Albuquerque, New Mexico 87102

C.E. Baum
Air Force Weapons Laboratory
Kirtland AFB, New Mexico 87117

Abstract

Scattering matrices of subshields and their norms have been used to relate the internal signals of an enclosed volume to the electromagnetic source environment. Both the line and aperture penetrations are included in the scattering matrix formulation. Experimental and analytical methods are proposed for the estimates of the scattering matrices. These methods can, in turn, be employed to analyze the overall shielding performance and to synthesize the subshield requirements of a system. An illustrative example is given in the discussion.

ACKNOWLEDGEMENTS

We wish to thank Dr. K.S.H. Lee of Dikewood, Lt. D. Andersh and Major J. Shuster of AFWL for their suggestions and interest in this problem.

PREFACE

"Now Yahweh came down to see the town and the tower that the sons of man had built. 'So they are all a single people with a single language!' said Yahweh. 'This is but the start of their undertakings! There will be nothing too hard for them to do. Come, let us go down and confuse their language on the spot so that they can no longer understand one another.' Yahweh scattered them thence over the whole face of the earth, and they stopped building the town. It was named Babel therefore, because there Yahweh confused the language of the whole earth. It was from there that Yahweh scattered them over the whole face of the earth."

(Genesis 11:5-9)

CONTENTS

CONTENTS

I. INTRODUCTION

It is an extremely complicated problem to analyze the overall shielding performance or to synthesize the shielding allocation requirement for an aeronautical system, since there are a large number of sensitive internal electronic components to be protected against electromagnetic interferences, such as those of nuclear electromagnetic pulse (NEMP) and lightning. One approach to analyze and synthesize such a problem has been developed in Reference 1 using the concept of electromagnetic topology and interaction sequence diagram, which eventually evolves into a supermatrix equation. Under certain practical assumptions, this supermatrix equation can be approximately solved, and the internal signals and their upperbounds are found to be related to the external electromagnetic environment and the shielding properties of shields. That is to say, with this approach the complicated problem is reduced to one of evaluating a set of environment and shield variables.

However, there are questions that remain to be answered regarding the approach. The electromagnetic penetration through a shield can be categorized as either a line or an aperture penetration (the diffusion penetration is less important and will not be included in this discussion). When the interaction sequence diagram is constructed, all the line and aperture penetration paths are modeled as "edges" with associated combined voltage waves (see Ref. 1). While the combined voltage waves can be easily defined along a line penetration path, there is no clear way to incorporate the field quantities along the aperture penetration path in the combined voltage formulation. One purpose of this report is to resolve this difficulty.

In order to use the above approach for shielding analysis and synthesis purposes, the environment and shield variables have to be calculated or measured in a way according to their definitions described by this approach. Unfortunately, most of the existing military standards for measuring the shielding performance do not satisfy these definitions. For example, each shielding variable in the approach is defined to be nearly independent of adjacent shields, whereas the shielding effectiveness measured according to MIL-STD-285 (see Ref. 2) varies a lot with the structure inside the shield.

Another purpose of this report is thus to establish certain rules for the preparation of future military standards to measure the shielding performance of an enclosure.

Section II of this report will summarize the approach of Reference 1 and give a method to resolve the difficulty in characterizing the aperture penetration. Section III will present an illustrative example. Section IV will explain how the shield and environment variables can be experimentally determined. Section V will demonstrate how the results in Sections II-IV can be used in the shielding design procedure for hardening an aeronautical system. Section VI will give recommendations for future developments to bring the supermatrix-norm approach to maturity.

II. BASIC CONSIDERATION

In a typical aeronautic system there are many electronic components, which are connected by wires or cables, exposed to electromagnetic interferences, either arriving from the outside (EMP, lightning) or are system generated (EMC, SGEMP). These interferences may damage or upset the components. To reduce the vulnerability one may try to reduce the electromagnetic coupling to the connecting wires and/or to limit the propagation of the interferences to the components (and/or, of course, to increase the components' damage or upset threshold). These protection schemes can be implemented with hardening fixes on surfaces separating one layer (or sublayer) from the other. In this section, certain parameters (or variables) characterizing the shielding surfaces will be defined, and the relationship of these parameters to the overall shielding performance will be discussed.

1. GENERAL DISCUSSION

In Reference 1, a supermatrix equation has been given for calculating the signal responses inside an aeronautic system due to an electromagnetic interference. The first step in the derivation of the supermatrix equation is to construct a topological diagram for the electronic system(for example, see Fig. 2.1a) and then to draw a corresponding interaction sequence diagram (see Fig. 2.1b). The interaction paths in the diagram include all the important penetration paths through apertures and along conducting wires. The vertices and edges of the interaction sequence diagram are similar to the junctions and tubes of a transmission-line network (Reference 3). Thus, a supermatrix equation similar to that obtained in Reference 3 for the transmission-line network can be obtained. That is, one has the following equation (with the tubes shrinking to zero length),

$$
\begin{aligned}
&[((1_{n,m})_{u,v})-((\tilde{S}_{n,m})_{u,v})] \odot ((\tilde{V}_n)_u) \\
&\quad \equiv ((\tilde{I}_{n,m})_{u,v}) \odot ((\tilde{V}_n)_u) \qquad (2.1) \\
&\quad = ((\tilde{S}_{n,m})_{u,v}) \odot ((\tilde{V}_{s_n})_u) \equiv ((\tilde{E}_n)_u)
\end{aligned}
$$

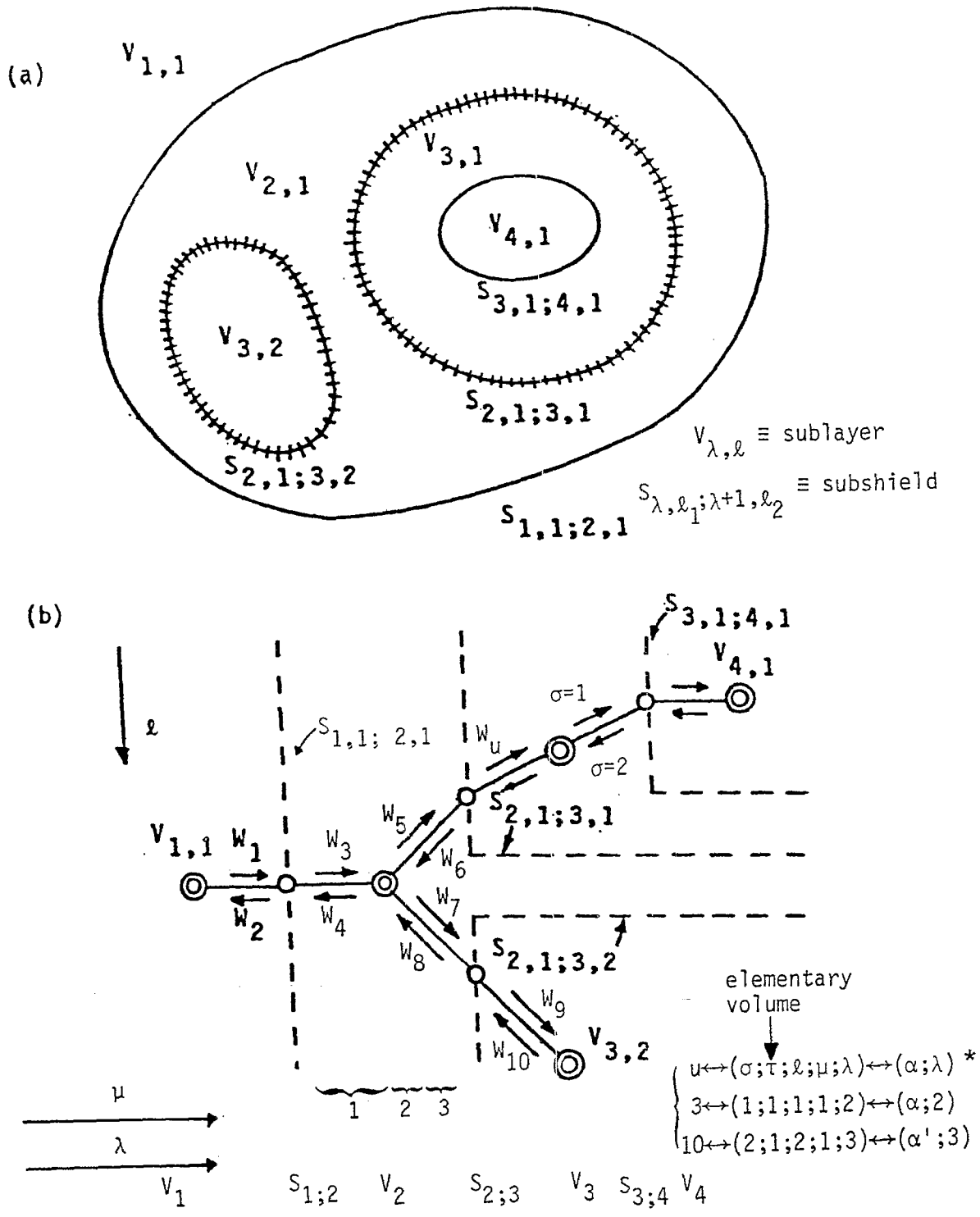

Figure 2.1. (a) A topological diagram, and (b) its corresponding interaction sequence diagram.

* For more partition examples, see Figure 3.1.

Here u and v, which can be further partitioned to correspond to the levels of the hierarchical topology (see Reference 1), are indices for the waves (W_u, W_v) on the edge (or tube) of the interaction sequence diagram (each edge has two waves propagating in opposite directions), and n, m are indices for the individual wire or penetration path inside the edges, and "~" is to indicate complex frequency-domain quantities, and "$\odot$" means generalized dot multiplication as defined by Equation 3.4 of Reference 1. A short description concerning how Equation 2.1 is derived is given in Appendix A. Also,

$((1_{n,m})_{u,v})$ ≡ identity supermatrix

$$((\tilde{I}_{n,m})_{u,v}) \equiv \text{interaction supermatrix} \equiv ((1_{n,m})_{u,v}) - ((\tilde{S}_{n,m})_{u,v}) \tag{2.2}$$

$((\tilde{S}_{n,m})_{u,v})$ ≡ scattering supermatrix with $(S_{n,m})_{u,v}$ scatters W_v wave into W_u wave

$((\tilde{E}_n)_u)$ ≡ source supervector

$$(\tilde{V}_n)_u \equiv \text{combined voltage vector of wave } W_u = (\tilde{V}_n^{(+)})_u + (\tilde{Z}_{c_{n,m}})_u \cdot (\tilde{I}_n^{(+)})_u \tag{2.3}$$

$$(\tilde{V}_{s_n})_u \equiv \text{combined voltage source vector for } W_u \equiv (\tilde{V}_{s_n}^{(+)})_u + (\tilde{Z}_{c_{n,m}})_u \cdot (\tilde{I}_{s_n}^{(+)})_u \tag{2.4}$$

$(\tilde{Z}_{c_{n,m}})_u$ ≡ normalization impedance matrix for W_u

$(\tilde{V}_n^{(+)})_u$, $(\tilde{I}_n^{(+)})_u$ ≡ true voltage and current vectors on the surface containing W_u with "+" indicating the current is positive in the propagating direction of W_u (see Figure 2.2)

(a)

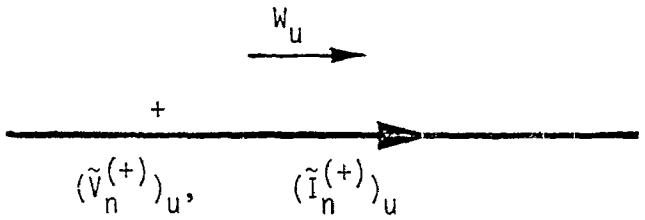

$$(\tilde{V}_n)_u = (\tilde{V}_n^{(+)})_u + (\tilde{Z}_{c_{n,m}})_u \cdot (\tilde{I}_n^{(+)})_u$$

(b)

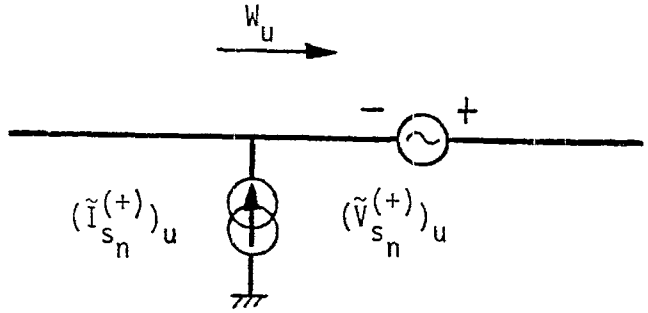

$$(\tilde{V}_{s_n})_u = (\tilde{V}_{s_n}^{(+)})_u + (\tilde{Z}_{c_{n,m}})_u \cdot (\tilde{I}_{s_n}^{(+)})_u$$

Figure 2.2. Sign conventions for the real voltages and currents used in the definitions of (a) the combined voltage, and (b) the combined source voltage.

$(\tilde{V}^{(+)}_{s_n})_u$, $(\tilde{I}^{(+)}_{s_n})_u$ ≡ voltage source vector and current source vectors for W_u, with "+" indicating that the voltage is positive when it increases with the propagating direction of W_u and the current is positive when it flows into the edge (see Fig. 2.2).

After solving for $((\tilde{V}_n)_u)$ from Equation 2.1, the "true" voltage and current can be obtained from the two combined voltage waves propagating through it.

To carry out the above calculation for a complex system is tedious and time-consuming. A more important practical approach is to introduce reasonable assumptions and approximations so that the equations can be simplified and the signal upperbounds inside the system can be estimated. In Reference 1, the good shielding approximation is used.

2. GOOD SHIELDING APPROXIMATION AND SIGNAL UPPERBOUNDS

Based on the structure of the identity and scattering supermatrices, the interaction supermatrix is block tridiagnal at the layer level of partition. That is, one has with indices λ, η for layers,

$$(\tilde{I}_{n,m})_{u,v} \equiv ((\tilde{I}_{n,m})_{\alpha,\beta})_{\lambda,\eta} = ((0_{n,m})_{\alpha,\beta})_{\lambda,\eta} \text{ , for } |\lambda-\eta| \geq 2, \qquad (2.5)$$

and with

$u \leftrightarrow \alpha,\lambda$, $v \leftrightarrow \beta,\eta$

When the combined voltage source vector $((\tilde{V}_{s_n})_\alpha)_\lambda$ is nonzero only in the outermost layer (λ=1), Equation 2.1 can be solved under the good shielding approximation. The good shielding approximation is imposed by assuming that the off-diagonal blocks of the interaction supermatrix are small in the norm sense (for a description of the norm concept, see References 4 and 5) compared to those of diagonal blocks. Physically, the good shielding approximation thus uses the assumption that the combined voltages of an outer layer are not influenced by those of its inner layers. The solution is, with the step by step procedure working from the bottom of the supermatrix equation,

$$((\tilde{V}_n)_\alpha)_\lambda \simeq (-1)((\tilde{I}_{n,m})_{\alpha,\beta})^{-1}_{\lambda,\lambda} \odot ((\tilde{I}_{n,m})_{\alpha,\beta})_{\lambda,\lambda-1} \odot$$

$$\odot ((\tilde{V}_n)_\alpha)_{\lambda-1}$$

$$\simeq (-1)^2((\tilde{I}_{n,m})_{\alpha,\beta})^{-1}_{\lambda,\lambda} \odot ((\tilde{I}_{n,m})_{\alpha,\beta})_{\lambda,\lambda-1} \odot$$

$$\odot ((\tilde{I}_{n,m})_{\alpha,\beta})^{-1}_{\lambda-1,\,\lambda-1} \odot ((\tilde{I}_{n,m})_{\alpha,\beta})_{\lambda-1,\,\lambda-2} \odot$$

$$\odot ((\tilde{V}_n)_\alpha)_{\lambda-2}$$

$$\simeq \text{----------}$$

$$\text{----------}$$

$$\simeq (-1)^{\lambda-1}((\tilde{I}_{n,m})_{\alpha,\beta})^{-1}_{\lambda,\lambda} \odot ((\tilde{I}_{n,m})_{\alpha,\beta})_{\lambda,\,\lambda-1} \odot \text{--------} \odot$$

$$\odot ((\tilde{I}_{n,m})_{\alpha,\beta})^{-1}_{2,2} \odot ((\tilde{I}_{n,m})_{\alpha,\beta})_{2,1} \odot$$

$$\odot ((\tilde{V}_n)_\alpha)_1$$

$$\simeq (-1)^{\lambda-1}((\tilde{I}_{n,m})_{\alpha,\beta})^{-1}_{\lambda,\lambda} \odot ((\tilde{I}_{n,m})_{\alpha,\beta})_{\lambda,\,\lambda-1} \odot \text{-------} \odot$$

$$\odot ((\tilde{I}_{n,m})_{\alpha,\beta})^{-1}_{2,2} \odot ((\tilde{I}_{n,m})_{\alpha,\beta})_{2,1} \odot$$

$$\odot ((\tilde{I}_{n,m})_{\alpha,\beta})^{-1}_{1,1} \odot ((\tilde{S}_{n,m})_{\alpha,\beta})_{1,1} \odot ((\tilde{V}_{s_n})_\alpha)_1 \qquad (2.6)$$

When the source vector is nonzero in an inner layer or in more than one layer, the complete solution can still be obtained using the above solution by applying superpositions and topological inversions (see Reference 6).

When there are decoupled sublayers within a layer the above approximate result can be carried one step further. In this case, one need only include interaction matrices associated with the paths connected between the interested sublayers in Equation 2.6 (see Reference 1).

From Equation 2.6, one can calculate the signal upperbounds using the norm concepts as follows.

$$\| ((\tilde{V}_n)_\alpha)_\lambda \| \leq \left\{ \sum_{\lambda'=0}^{\lambda-2} \| ((\tilde{I}_{n,m})_{\alpha,\beta})^{-1}_{\lambda-\lambda',\lambda-\lambda'} \| \; \| ((\tilde{I}_{n,m})_{\alpha,\beta})_{\lambda-\lambda',\lambda-\lambda'-1} \| \right\} \tag{2.7}$$

$$\| ((\tilde{I}_{n,m})_{\alpha,\beta})^{-1}_{1,1} \| \quad \| ((\tilde{S}_{n,m})_{\alpha,\beta})_{1,1} \| \quad \| ((\tilde{V}_{s_n})_\alpha)_1 \|$$

Various vector and its induced natural matrix norms can be used, depending on what the quantity of interest is. For example, if the current or voltage upperbound on an individual wire is desired, one should use the maximum norm (Hölder norm with $p \to \infty$); if the maximum energy transferred to a volume is desired, one should use the Euclidean norm (p=2) (see the last formula of Equation 2.8). If the quantity is intended for assessing a black box by comparing with a "black box failure norm", then the 1-norm ($\| \|_1$) should be used (see Reference 7). For the maximum ($\| \|_\infty$) and Enclidean ($\| \|_2$) norms, one needs only to consider the 2-norms for the terms on the right-hand side of Equation 2.7 because $\| ((\tilde{V}_n)_\alpha)_\lambda \|_\infty \leq \| ((\tilde{V}_n)_\alpha)_\lambda \|_2$, unless the maximum norms give a tighter upperbound and are easier to calculate.

The properties of matrix and vector norms can be found in References 4 and 5. Some useful properties for the following discussion are given below.

$$\| \left((1_{n,m})-(A_{n,m})\right)^{-1} \| \leq \begin{cases} \left\{1-\| (A_{n,m}) \|\right\}^{-1}, & \text{if } \|(A_{n,m})\| \leq 1 \\ \| (A_{n,m})^{-1} \| \left\{1-\| (A_{n,m})^{-1} \| \right\}^{-1}, & \text{if } \| (A_{n,m})^{-1} \| \leq 1 \end{cases}$$

$$
\begin{aligned}
\| (A_{n,m}) \|_{\infty} &= \max_{n} \sum_{m} |A_{n,m}| \\
\| (A_{n,m}) \|_{2} &= [\rho\{(A_{n,m})^{\dagger} \cdot (A_{n,m})\}]^{1/2} \\
\| (V_{n}) \|_{p} &= \left\{ \sum_{n} |V_{n}|^{p} \right\}^{1/p} \\
&= \max_{n} \{ |V_{n}| \}, \text{ for } p \to \infty
\end{aligned}
\tag{2.8}
$$

where "†" represents the conjugate transpose and $\rho\{\}$ means the spectral radius. Certain norm relations derived from the above equation, which are particularly useful for the scattering supermatrix considerations can be found in Reference 8.

Having derived Equations 2.6 and 2.7, one can quantitatively consider the influence of each block matrix on the signal response. The diagonal block matrices (the inverse matrices) contain the information on the reflection coefficients of the shields. The off-diagonal block matrices bear the signatures of the transmission coefficients of the shields and are the main quantities to reduce internal signals. Since the off-diagonal block matrices are essentially constructed from the transmission coefficients of various POEs, the first step is to evaluate the various POE transmission coefficients. For a line POE the evaluation of the transmission (reflection) coefficient is straightforward. For an aperture POE the evaluation of its transmission coefficients requires further consideration.

3. SCATTERING MATRIX FOR APERTURE PENETRATION

One way to bypass the difficulty of evaluating the scattering matrix elements associated with aperture penetrations is to neglect the less important field-to-field interaction. In doing this, all the edges in the interaction sequence diagram, except those belonging to the outermost layer, are the conducting wires. The more important field-to-wire (which will be considered only for the outermost shield) and wire-to-wire interactions through an aperture can be taken into account by introducing additional sources on the wires in the inner layer. The effect of these

additional sources can be shown to be equivalent to the introduction of appropriate scattering (transmission) matrices. To elaborate this point further consider the two interaction mechanisms separately.

a. Wire-to-wire interaction through aperture--First, consider Figure 2.3a in which the subshield has an aperture in it and the wires interact through the aperture. To calculate the aperture transmission coefficient, consider Figure 2.3b, the equivalent circuit of Figure 2.3a for the inner wire when the inner wire has only the outgoing wave. From Figure 2.3b one has

$$\tilde{S}_{\beta,\alpha;\lambda+1,\lambda} = \frac{\tilde{V}^{(+)}_{\beta\,;\,\lambda+1} + \tilde{Z}_{C_{\beta;\lambda+1}} \tilde{I}^{(+)}_{\beta\,;\,\lambda+1}}{\tilde{V}^{(+)}_{\alpha\,;\,\lambda} + \tilde{Z}_{C_{\alpha;\lambda}} \tilde{I}^{(+)}_{\alpha\,;\,\lambda}}$$

$$= \frac{2\,\tilde{Z}_{C_{\beta;\lambda+1}}}{\tilde{Z}_{C_{\beta;\lambda+1}} + \tilde{Z}_{L_{\beta;\lambda+1}}} \quad \frac{\tilde{V}^{(+)}_{s_{\lambda+1}} + \tilde{Z}_{L_{\beta;\lambda+1}} \tilde{I}^{(+)}_{s_{\lambda+1}}}{\tilde{V}^{(+)}_{\alpha\,;\,\lambda} + \tilde{Z}_{C_{\alpha;\lambda}} \tilde{I}^{(+)}_{\alpha;\lambda}} \tag{2.9}$$

$$= \frac{2\,\tilde{Z}_{C_{\beta;\lambda+1}}}{\tilde{Z}_{C_{\beta;\lambda+1}} + \tilde{Z}_{L_{\beta;\lambda+1}}} \quad \frac{\tilde{Z}_{C_{\alpha;\lambda}}}{\tilde{Z}_{L_{\alpha;\lambda}} + \tilde{Z}_{C_{\alpha;\lambda}}} \quad \frac{\tilde{V}^{(+)}_{s_{\lambda+1}}}{\tilde{Z}_{C_{\alpha;\lambda}} \tilde{I}^{(+)}_{\alpha;\lambda}}$$

$$+ \frac{2\,\tilde{Z}_{L_{\beta;\lambda+1}}}{\tilde{Z}_{C_{\beta;\lambda+1}} + \tilde{Z}_{L_{\beta;\lambda+1}}} \quad \frac{\tilde{Z}_{L_{\alpha;\lambda}}}{\tilde{Z}_{L_{\alpha;\lambda}} + \tilde{Z}_{C_{\alpha;\lambda}}} \quad \frac{\tilde{Z}_{C_{\beta;\lambda+1}} \tilde{I}^{(+)}_{s_{\lambda+1}}}{\tilde{V}^{(+)}_{\alpha;\lambda}}$$

For the transmission coefficient upperbound, the quantity of interest, one has

$$|\tilde{S}_{\beta,\alpha;\lambda+1,\lambda}| \leq \max \left\{ 2|\tilde{v}_{s_{\lambda+1,\lambda}}|; 2|\tilde{i}_{s_{\lambda+1,\lambda}}| \right\} \tag{2.10}$$

after using the condition that $\tilde{Z}_{C_{\beta;\lambda+1}}$ and $\tilde{Z}_{C_{\alpha;\lambda}}$ have small imaginary parts, and

(a)

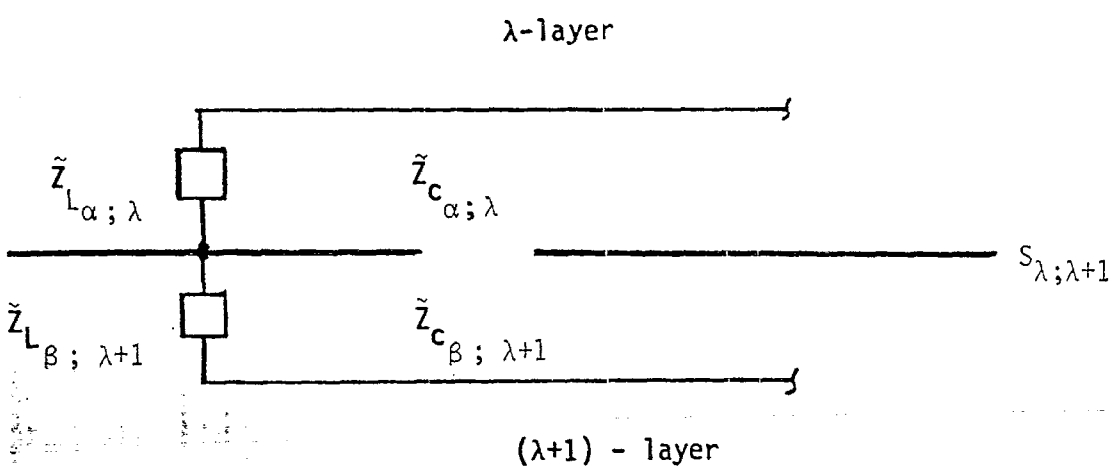

Note; The indices n,m have been omitted, because only one wire in each layer is assumed.

(b)

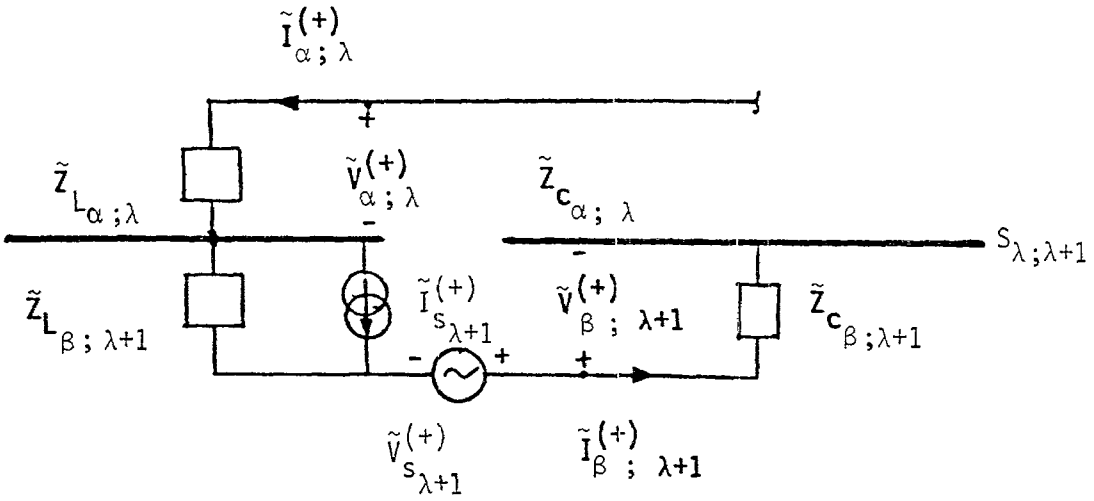

$$\tilde{V}^{(+)}_{s_{\lambda+1}} = \tilde{v}_{s_{\lambda+1},\lambda} \tilde{Z}_{C_{\alpha;\lambda}} \tilde{I}^{(+)}_{\alpha;\lambda} \; (= s\,\tilde{\Phi}_m)$$

$$\tilde{Z}_{C_{\beta;\lambda+1}} \tilde{I}^{(+)}_{s_{\lambda+1}} = \tilde{i}_{s_{\lambda+1},\lambda} \tilde{V}^{(+)}_{\alpha;\lambda} \text{ (where } \tilde{I}^{(+)}_{s_{\lambda+1}} = s\,\tilde{\Phi}_e)$$

$\tilde{\Phi}_m$ = magnetic flux linking wire

$\tilde{\Phi}_e$ = electric charge deposited on wire

Figure 2.3. (a) Schematic drawing of wires interacting through an aperture, and (b) its equivalent circuit for the inner wire when the inner wire allows only outgoing waves.

$$\tilde{v}_{s_{\lambda+1,\lambda}} = \tilde{V}^{(+)}_{s_{\lambda+1}} \Big/ \left[\tilde{Z}_{c_{\alpha;\lambda}} \tilde{I}^{(+)}_{\alpha;\lambda}\right] ; \quad \tilde{i}_{s_{\lambda+1,\lambda}} = \left[\tilde{Z}_{c_{\beta;\lambda+1}} \tilde{I}^{(+)}_{s_{\lambda+1}}\right] \Big/ \tilde{V}^{(+)}_{\alpha;\lambda} \tag{2.10a}$$

With Equation 2.10, one can essentially treat the wire-to-wire aperture interaction as the line penetration. When the wires are not involved in the "real" line penetration, Equation 2.10 gives the estimate of the transmission coefficient for the wire-to-wire interaction. In the case that the wires interact through more than one aperture and also through the real line penetration, one should combine all penetration effects together. The transmission coefficient upperbound for this case is

$$|\tilde{S}_{\beta,\alpha;\lambda+1,\lambda}| \leq |\tilde{S}^{(L)}_{\beta,\alpha;\lambda+1,\lambda}| + \sum_i \max \left\{2|\tilde{v}^{(i)}_{s_{\lambda+1,\lambda}}| ; 2|\tilde{i}^{(i)}_{s_{\lambda+1,\lambda}}|\right\} \tag{2.11}$$

where the superscript (L) indicates that the quantity is for the line penetration and (i) is the index for the apertures. As for the reflection coefficients in the subshield scattering matrix, under the good shielding approximation and the condition that the wires are outside the exclusion regions, their values should not be changed appreciably by the aperture. An exclusion region is designated for the purpose of good shielding practice and does not allow wires residing in it. The upperbound estimate using Equation 2.11 can be used to obtain the appropriate scattering matrix and its norm when more than one wire on either and/or both sides of the shield are involved in the interaction process.

The above transmission coefficient derivation is to be used for a wave definition so that the magnitude (or norm) of the combined voltage of the incoming wave in the outer layer is not smaller than that of the outgoing wave. This will further be clarified in Appendix B where an alternative definition of the transmission matrix is given.

b. Field-to-wire interaction through aperture--To treat the field-to-wire interaction through an aperture consider the geometry depicted in

Figure 2.4a. In this figure, there is an aperture in shield $S_{1;2}$. The field in the outer layer (V_1) will induce equivalent sources on the internal wire (Figure 2.4b). The effect of the equivalent sources can, in turn, be expressed in terms of an appropriate transmission coefficient.

In order to fit into the general interaction supermatrix formulation, the transmission coefficient has to be calculated as the ratio of the combined voltages of the internal outgoing wave to the external incoming wave. The combined voltage for the external electric and magnetic fields is yet to be defined. For an electrically small aperture, the electric and magnetic field interactions with an internal wire are independent of each other. Although the choice of a normalization impedance for the combined voltage definition is artifical in this case, the natural choice is the free space wave impedance. $Z_0 = \sqrt{\mu_0/\varepsilon_0} \simeq 120\ \pi \simeq 377\Omega$. With the normalization impedance of Z_0 and the introduction of a length normalization factor "a", an "imaginary" wire can be created for the electric and magnetic fields. The wire configuration is shown in Figure 2.5a. This is analogous to a plane wave incident at an angle. A possible alternative is given in Figure 2.5b. This, on the other hand, simulates a plane wave propagating parallel to the surface. Both configurations give a combined voltage of $a[\tilde{E}_{sc} + Z_0 \tilde{H}_{sc}]$ for the incoming waves at the shield, and will give the same internal signal responses. This imaginary wire can further be assumed to be non-interacting with other external wires. The effect of the interaction between the field and other external wires is taken care of by introducing appropriate sources on other external wires.

From Figure 2.4b and the above combined voltage definition, the transmission coefficient for the field-to-wire aperture interaction can be estimated as follows (take $\lambda = 1$).

$$\tilde{S}_{\beta,\alpha;2,1} = \frac{\tilde{V}^{(+)}_{\beta\,;\,2} + \tilde{Z}_{c_{\beta;\,2}}\,\tilde{I}^{(+)}_{\beta;2}}{a[\tilde{E}_{sc} + Z_0\,\tilde{H}_{sc}]} \tag{2.12}$$

$$= \frac{2\,\tilde{Z}_{c_{\beta;2}}}{\tilde{Z}_{c_{\beta;2}} + \tilde{Z}_{L_{\beta;2}}} \quad \frac{\tilde{V}^{(f)}_{s_2} + \tilde{Z}_{L_{\beta;2}}\,\tilde{I}^{(f)}_{s_2}}{a[\tilde{E}_{sc} + Z_0\,\tilde{H}_{sc}]}$$

(a)

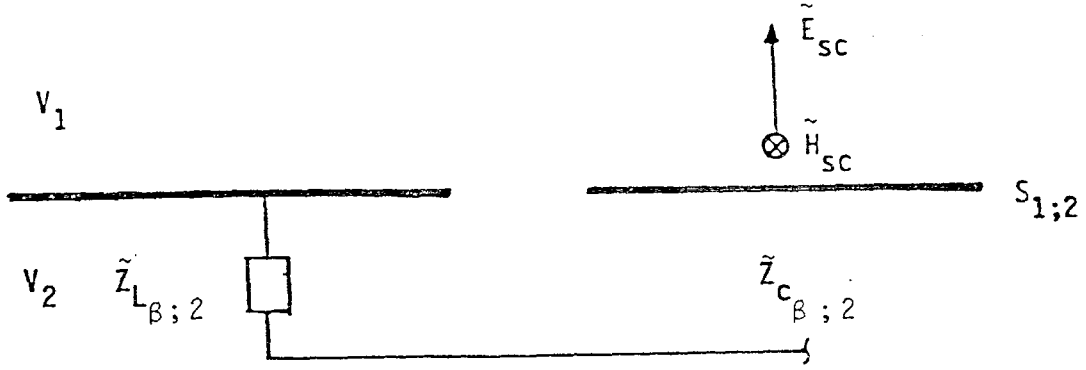

Note: The indices n,m have been omitted, because there is only one wire in V_2.

(b)

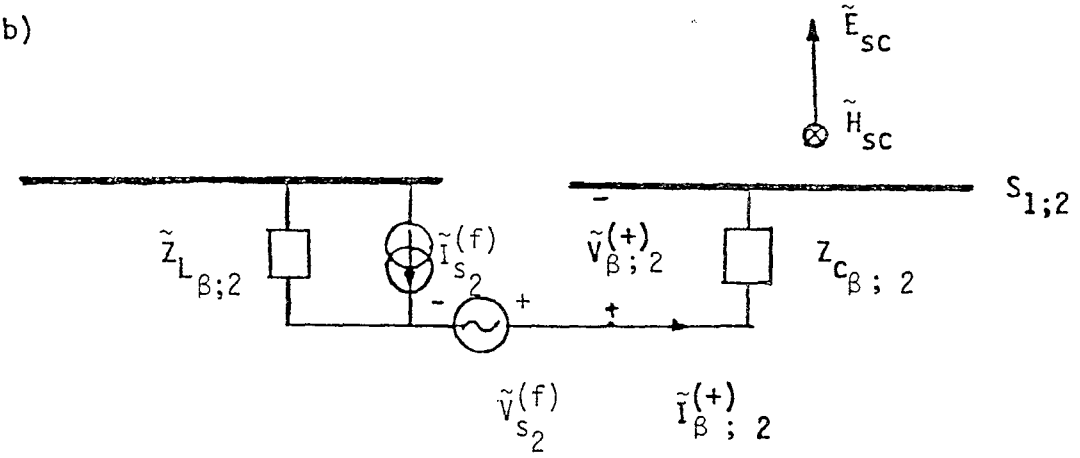

$$\tilde{V}^{(f)}_{s_2} = \tilde{v}^{(f)}_{s_{2,1}} [aZ_o \tilde{H}_{sc}] \; (= s\,\tilde{\Phi}^{(f)}_m)$$

$$\tilde{Z}_{C_{\beta;2}} \tilde{I}^{(f)}_{s_2} = \tilde{i}^{(f)}_{s_{2,1}} [a\tilde{E}_{sc}] \; (\text{where } \tilde{I}^{(f)}_{s_2} = s\,\tilde{\Phi}^{(f)}_e)$$

$\tilde{E}_{sc}$, $\tilde{H}_{sc}$ = short-circuited electric, magnetic fields when the aperture is covered with conductor

$\tilde{\Phi}^{(f)}_m$ = magnetic flux linking wire due to $\tilde{H}_{sc}$

$\tilde{\Phi}^{(f)}_e$ = electric charge depoisited on wire due to $\tilde{E}_{sc}$

Figure 2.4. (a) Schematic drawing of a field interacting with a wire through an aperture, and (b) its equivalent circuit for the inner wire when the inner wire allows only outgoing waves.

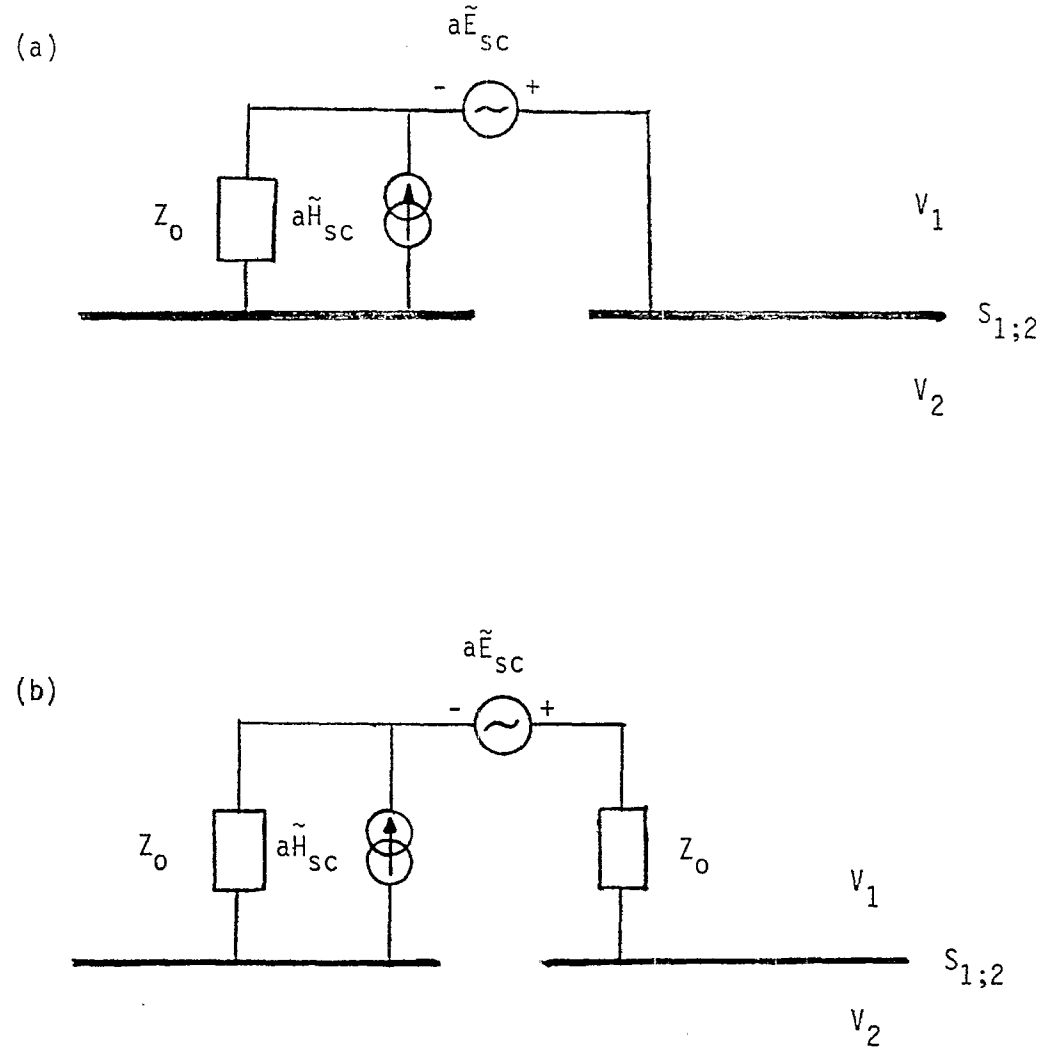

Figure 2.5. Two examples of the "imaginary" wire configurations created for the electric and magnetic fields.

$$= \frac{2\,\tilde{Z}_{c_{\beta;2}}}{\tilde{Z}_{c_{\beta;2}} + \tilde{Z}_{L_{\beta;2}}} \; \frac{a\,Z_o\,\tilde{H}_{sc}}{a\left[\tilde{E}_{sc} + Z_o\tilde{H}_{sc}\right]} \; \frac{\tilde{V}^{(f)}_{s_2}}{a\,Z_o\tilde{H}_{sc}}$$

$$+ \frac{2\,\tilde{Z}_{L_{\beta;2}}}{\tilde{Z}_{c_{\beta;2}} + \tilde{Z}_{L_{\beta;2}}} \; \frac{a\,\tilde{E}_{sc}}{a\left[\tilde{E}_{sc} + Z_o\tilde{H}_{sc}\right]} \; \frac{\tilde{Z}_{c_{\beta;2}}\,\tilde{I}^{(f)}_{s_2}}{a\,\tilde{E}_{sc}} \qquad (2.12)$$

Here, the index α has been assigned for the incoming wave on the "imaginary" field wire, and the superscript (f) for quantities corresponding to field interaction. To proceed further in the estimate of the transmission coefficient upperbound, one takes $\tilde{E}_{sc}$ and $\tilde{H}_{sc}$ so that

$$\frac{|\,a\,Z_o\,\tilde{H}_{sc}\,|}{|\,a\left[\tilde{E}_{sc} + Z_o\,\tilde{H}_{sc}\right]\,|} \leq 1; \quad \frac{|\,a\,\tilde{E}_{sc}\,|}{|\,a\left[\tilde{E}_{sc} + Z_o\,\tilde{H}_{sc}\right]\,|} \leq 1 \qquad (2.12b)$$

These conditions are not required if the scattering matrix is defined by using both $a\left[\tilde{E}_{sc} + Z_o\tilde{H}_{sc}\right]$ and $a\left[\tilde{E}_{sc} - Z_o\tilde{H}_{sc}\right]$ for the external combined voltages, as described in Appendix B. One then has

$$|\,\tilde{S}_{\beta,\alpha;2,1}\,| \leq \max\,\{2|\,\tilde{v}^{(f)}_{s_{2,1}}\,|\,;\; 2|\,\tilde{i}^{(f)}_{s_{2,1}}\,|\} \qquad (2.13)$$

where

$$\tilde{v}^{(f)}_{s_{2,1}} = \tilde{V}^{(f)}_{s_2} \;/\; [a\,Z_o\,\tilde{H}_{sc}]$$

$$\tilde{i}^{(f)}_{s_{2,1}} = \tilde{Z}_{c_{\beta;2}}\,\tilde{I}^{(f)}_{s_2} \;/\; [a\,\tilde{E}_{sc}] \qquad (2.13b)$$

Equation 2.13 can give a transmission coefficient upperbound for the field-to-wire aperture interaction when the wires are placed immediately outside the exclusion regions. Again, for $|\tilde{i}_s^{(f)}|$ the upperbound depends on the size of the internal wire. A "maximum" upperbound can be obtained by using a bowl instead of a wire for the internal circuit. Equation 2.13 can be used for calculating the scattering matrix and its norm when there is more than one wire and more than one aperture involved in the interaction process. In the case that the internal wire goes in both directions away from the aperture, the single wire should be treated as two wires, similar to that given in Appendix B where an alternative transmission coefficient definition for the aperture penetration is given.

4. SOURCE VECTORS

It is appropriate at this point to discuss the configuration for the outermost layer, especially the source vectors. For field penetration through an aperture, the circuits for the "imaginary" wire are given in Figure 2.5. Similar circuits can also be obtained for a wire exposed to a source environment. The wire acts as an antenna on which voltages and/or currents can be induced. To the connected shield and internal wires the effect of the antenna can be represented by either a Thevenin or Norton equivalent circuit (see Figure 2.6). With the introduction of an appropriate normalization impedance, the circuit can be easily incorporated into the supermatrix formulation for estimation of the associated source vectors and scattering matrix elements.

The circuit elements in the equivalent circuits of Figure 2.6 can be analytically or experimentally determined. Their values will depend on the source environment and the wire structure. The techniques for their determination and the results for certain special antenna structures can be found in several books and papers (for example, see Reference 9).

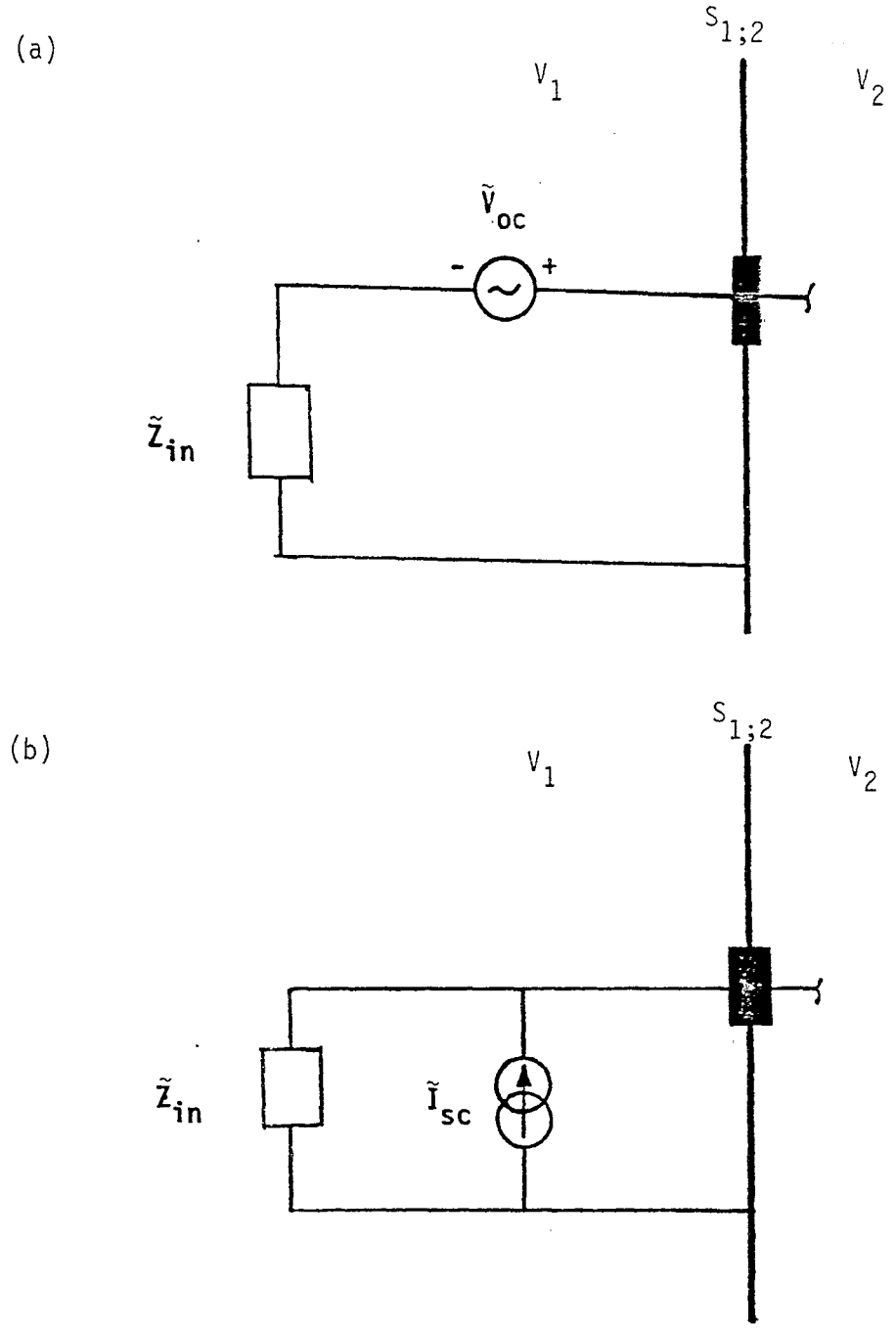

Figure 2.6. (a) Thevénin and (b) Norton equivalent circuits for a protruded wire exposed to an electromagnetic source.

III. AN ILLUSTRATIVE EXAMPLE

An illustrative example will be given in this section to demonstrate how the basic ideas described in Section II can be used. The topological diagram of the example is depicted in Figure 3.1a. This example has a relative shielding order of 2 (see Reference 6), and is therefore relatively simple. Nevertheless, the demonstration can be easily extended to a more complicated system. The exterior layer (V_1) in the example corresponds to the location of various important electromagnetic interference sources, such as EMP, lightning, etc. The innermost layer (V_3) contains sensitive and critical electronics. Of course, the innermost layer can also include strong interference sources (such as transmitting equipment) and equipment carrying signals that are not intended to be detected in the exterior layer. In this case, a topological inversion can be applied to transform the innermost layer to exterior and vice versa, so that a similar topological diagram can be obtained. For this reason, only the case with an electromagnetic interference source in the exterior layer need be discussed.

1. GENERAL SOLUTION

From Figure 3.1a, it is observed that both shields allow aperture and line penetrations. From the locations of the penetration point it is observed that the aperture penetrations are important only through field-wire interation for the outer shield, and through wire-to-wire interaction for the inner shield. A corresponding interaction sequence diagram is given in Figure 3.1b which shows that there are either two or one tubes in each layer and two combined voltage waves propagating on each tube. Except for the outermost tube which includes two wires, one real wire and one imaginary wire to represent the external electric and magnetic field penetration, each tube has only one wire. Using the sign convention, symbol definitions and formulas of Section II, one has

$$\left(\left(\left(\tilde{I}_{n,m}\right)_{\alpha,\beta}\right)_{\lambda,n}\right) \odot \left(\left(\left(\tilde{V}_n\right)_\alpha\right)_\lambda\right) = \left(\left(\left(\tilde{E}_n\right)_\alpha\right)_\lambda\right) \tag{3.1}$$

where

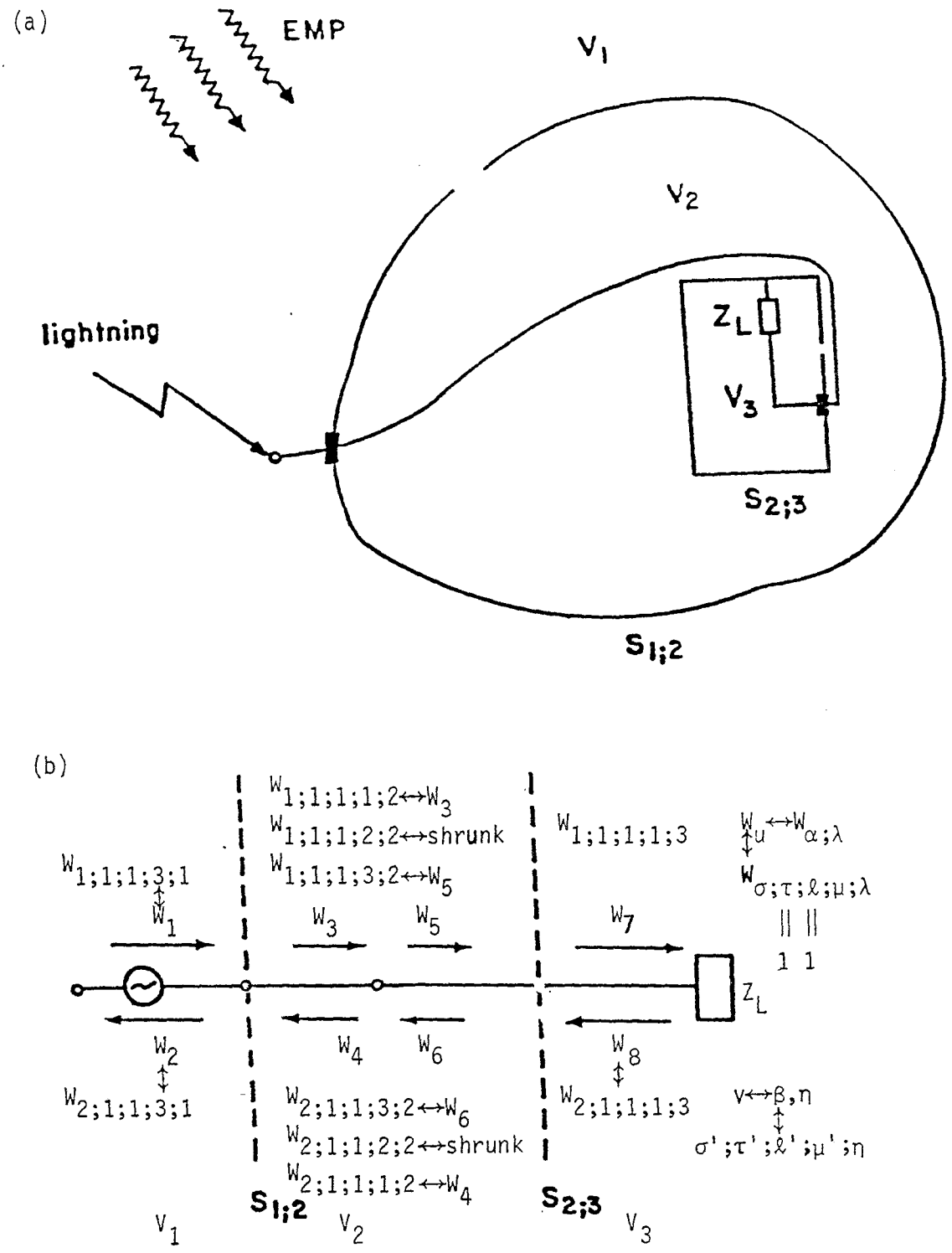

Figure 3.1. (a) The topological diagram, and (b) its corresponding interaction sequence diagram for the simple illustrative example.

$$\left(\left(\left(\tilde{I}_{n,m}\right)_{\alpha,\beta}\right)_{\lambda,\eta}\right) \equiv \left(\left(\left(1_{n,m}\right)_{\alpha,\beta}\right)_{\lambda,\eta}\right) - \left(\left(\left(\tilde{S}_{n,m}\right)_{\alpha,\beta}\right)_{\lambda,\eta}\right)$$

$$\equiv \begin{pmatrix} \left(\left(\tilde{I}_{n,m}\right)_{\alpha,\beta}\right)_{1,1} & \left(\left(\tilde{I}_{n,m}\right)_{\alpha,\beta}\right)_{1,2} & \left(\left(\tilde{I}_{n,m}\right)_{\alpha,\beta}\right)_{1,3} \\ \left(\left(\tilde{I}_{n,m}\right)_{\alpha,\beta}\right)_{2,1} & \left(\left(\tilde{I}_{n,m}\right)_{\alpha,\beta}\right)_{2,2} & \left(\left(\tilde{I}_{n,m}\right)_{\alpha,\beta}\right)_{1,3} \\ \left(\left(\tilde{I}_{n,m}\right)_{\alpha,\beta}\right)_{3,1} & \left(\left(\tilde{I}_{n,m}\right)_{\alpha,\beta}\right)_{3,2} & \left(\left(\tilde{I}_{n,m}\right)_{\alpha,\beta}\right)_{3,3} \end{pmatrix} \qquad (3.2)$$

$$= \left(\begin{array}{cccc|cccc|cc} 1 & 0 & -[\tilde{S}_{11}]_{1,2} & 0 & 0 & 0 & 0 & 0 & 0 & 0 \\ 0 & 1 & 0 & -[\tilde{S}_{22}]_{1,2} & 0 & 0 & 0 & 0 & 0 & 0 \\ -[\tilde{S}_{11}]_{2,1} & 0 & 1 & 0 & 0 & -[\tilde{S}_1]_{2,4} & 0 & 0 & 0 & 0 \\ 0 & -[\tilde{S}_{22}]_{2,1} & 0 & 1 & 0 & -[\tilde{S}_2]_{2,4} & 0 & 0 & 0 & 0 \\ \hline -[\tilde{S}_1]_{3,1} & -[\tilde{S}_2]_{3,1} & 0 & 0 & 1 & -\tilde{S}_{3,4} & 0 & 0 & 0 & 0 \\ 0 & 0 & 0 & 0 & 0 & 1 & 0 & -1 & 0 & 0 \\ 0 & 0 & 0 & 0 & -1 & 0 & 1 & 0 & 0 & 0 \\ 0 & 0 & 0 & 0 & 0 & 0 & -\tilde{S}_{6,5} & 1 & 0 & -\tilde{S}_{6,8} \\ \hline 0 & 0 & 0 & 0 & 0 & 0 & -\tilde{S}_{7,5} & 0 & 1 & -\tilde{S}_{7,8} \\ 0 & 0 & 0 & 0 & 0 & 0 & 0 & 0 & -\tilde{S}_{8,7} & 1 \end{array}\right)$$

$$\underbrace{\underbrace{m=1 \quad m=2}_{v=1} \quad \underbrace{m=1 \quad m=2}_{v=2}}_{\sigma'=1 \qquad \sigma'=2}$$

$$\mu'=3,\ell'=1,\tau'=1$$

$$\eta=1$$

$$\underbrace{\underbrace{v=3 \quad v=4}_{\sigma'=1 \quad \sigma'=2} \quad \underbrace{v=5 \quad v=6}_{\sigma'=1 \quad \sigma'=2}}_{\mu'=1 \qquad \mu'=3} \quad \underbrace{\underbrace{v=7 \quad v=8}_{\sigma'=1 \quad \sigma'=2}}_{\mu'=1}$$

$$\ell'=1,\tau'=1 \qquad \ell'=1,\tau'=1$$

$$\eta=2 \qquad \eta=3$$

where $\alpha,\beta \leftrightarrow \sigma,\sigma';\ \tau,\tau';\ell,\ell';\mu,\mu'$

$$\left(\left(\left(\tilde{V}_n\right)_\alpha\right)_\lambda\right) \equiv \begin{pmatrix} \left(\left(\tilde{V}_n\right)_\alpha\right)_1 \\ \left(\left(\tilde{V}_n\right)_\alpha\right)_2 \\ \left(\left(\tilde{V}_n\right)_\alpha\right)_3 \end{pmatrix} = \begin{pmatrix} [\tilde{V}_1]_1 \\ [\tilde{V}_2]_1 \\ [\tilde{V}_1]_2 \\ [\tilde{V}_2]_2 \\ \text{-----} \\ \tilde{V}_3 \\ \tilde{V}_4 \\ \tilde{V}_5 \\ \tilde{V}_6 \\ \text{-----} \\ \tilde{V}_7 \\ \tilde{V}_8 \end{pmatrix} \tag{3.3}$$

$$\left(\left(\left(\tilde{E}_n\right)_\alpha\right)_\lambda\right) \equiv \left(\left(\left(\tilde{S}_{n,m}\right)_{\alpha,\beta}\right)_{\lambda,n}\right) \odot \left(\left(\left(\tilde{V}_{s_n}\right)_\alpha\right)_\lambda\right)$$

or

$$\begin{pmatrix} \left(\left(\tilde{E}_n\right)_\alpha\right)_1 \\ \left(\left(\tilde{E}_n\right)_\alpha\right)_2 \\ \left(\left(\tilde{E}_n\right)_\alpha\right)_3 \end{pmatrix} \equiv \left(\left(\left(\tilde{S}_{n,m}\right)_{\alpha,\beta}\right)_{\lambda,n}\right) \odot \begin{pmatrix} \left(\left(\tilde{V}_{s_n}\right)_\alpha\right)_1 \\ \left(\left(\tilde{V}_{s_n}\right)_\alpha\right)_2 \\ \left(\left(\tilde{V}_{s_n}\right)_\alpha\right)_3 \end{pmatrix} \tag{3.4}$$

and

$$\left(\left(\tilde{V}_{s_n}\right)_\alpha\right)_1 = \left(\begin{pmatrix} [\tilde{V}_{s_1}]_1 \\ [\tilde{V}_{s_2}]_1 \end{pmatrix}, \begin{pmatrix} [\tilde{V}_{s_1}]_2 \\ [\tilde{V}_{s_2}]_2 \end{pmatrix}\right), \quad \left(\left(\tilde{V}_{s_n}\right)_\alpha\right)_2 = \begin{pmatrix} 0 \\ 0 \\ 0 \\ 0 \end{pmatrix}, \quad \left(\left(\tilde{V}_{s_n}\right)_\alpha\right)_3 = \begin{pmatrix} 0 \\ 0 \end{pmatrix} \tag{3.5}$$

where, in order to have the simple representation of Equations 3.2, 3.3 and 3.4, the n,m indices (inside the square brackets) are used only for the wires in the outermost layer, and the indices outside the square brackets and those unbracketed variables are referred to the waves, i.e., in

$$[\tilde{A}_x]_*,\ [\tilde{A}_{x,x}]_{*,*},\ [\tilde{A}_x]_{*,*},\ \tilde{A}_{*,*},\ \tilde{A}_*$$

x,*, are respectively referred to the wire index (n or m) in the outermost layer and the wave index (u or v). The corresponding partitioned indices according to the levels of the hierachical topology are given in Figure 3.1b. Here, the zero-tube-length assumption has been used, and hence the layer propagation matrices are identity matrices. For a tighter bound estimate, one should include suitable delay and/or decay factors in the above formulation.

2. GOOD SHIELDING APPROXIMATION AND SIGNAL UPPERBOUND

After imposing the good shielding assumption, the approximate solution to Equation 3.1 is explicitly given by

$$\begin{aligned}\left(\left(\tilde{V}_n\right)_\alpha\right)_3 \simeq\ & \left(\left(\tilde{I}_{n,m}\right)_{\alpha,\beta}\right)^{-1}_{3,3} \odot \left(\left(\tilde{I}_{n,m}\right)_{\alpha,\beta}\right)_{3,2} \odot \left(\left(\tilde{I}_{n,m}\right)_{\alpha,\beta}\right)^{-1}_{2,2} \\ & \odot \left(\left(\tilde{I}_{n,m}\right)_{\alpha,\beta}\right)_{2,1} \odot \left(\left(\tilde{I}_{n,m}\right)_{\alpha,\beta}\right)^{-1}_{1,1} \odot \left(\left(\tilde{S}_{n,m}\right)_{\alpha,\beta}\right)_{1,1} \odot \left(\left(\tilde{V}_{s_n}\right)_\alpha\right)_1\end{aligned} \tag{3.6}$$

from which the norm relationship suitable for bounding the internal signal is

$$\| \left((\tilde{V}_n)_\alpha\right)_3 \| \leq \| \left((\tilde{I}_{n,m})_{\alpha,\beta}\right)^{-1}_{3,3} \| \, \| \left((\tilde{I}_{n,m})_{\alpha,\beta}\right)_{3,2} \| \, \| \left((\tilde{I}_{n,m})_{\alpha,\beta}\right)^{-1}_{2,2} \|$$
$$\| \left((\tilde{I}_{n,m})_{\alpha,\beta}\right)_{2,1} \| \, \| \left((\tilde{I}_{n,m})_{\alpha,\beta}\right)^{-1}_{1,1} \| \, \| \left((\tilde{S}_{n,m})_{\alpha,\beta}\right)_{1,1} \| \, \| \left((\tilde{V}_{s_n})_\alpha\right)_1 \| \tag{3.7}$$

As mentioned in Section II, there are various methods to obtain bounds for the norms in the above equation. The most straightforward method is to consider the 2-norms for the terms on the right-hand side of Equation 3.7. From this consideration, one has

$$\| \left((\tilde{V}_n)_\alpha\right)_3 \|_\infty \leq \| \left((\tilde{V}_n)_\alpha\right)_3 \|_2 \leq \frac{\| \left((\tilde{S}_{n,m})_{\alpha,\beta}\right)_{3,2} \|_2}{1 - \| \left((S_{n,m})_{\alpha,\beta}\right)_{3,3} \|_2} \cdot \frac{\| \left((\tilde{S}_{n,m})_{\alpha,\beta}\right)_{2,1} \|_2}{1 - \| \left((\tilde{S}_{n,m})_{\alpha,\beta}\right)_{2,2} \|_2}$$
$$\cdot \frac{\| \left((\tilde{S}_{n,m})_{\alpha,\beta}\right)_{1,1} \|_2}{1 - \| \left((\tilde{S}_{n,m})_{\alpha,\beta}\right)_{1,1} \|_2} \cdot \| \left((\tilde{V}_{s_n})_\alpha\right)_1 \|_2 \tag{3.8}$$

To obtain Equ. 3.8, $(\tilde{I}) = (1) - (\tilde{S})$, $\|(\tilde{S})_{\lambda,\lambda}\|_2 < 1$, and the first equation of Equ. 2.8 have been used. $\|(\tilde{S})_{\lambda,\lambda}\|_2 < 1$ is true under certain restrictive conditions, such as when $(\tilde{Z}_c)_\lambda$ is a diagonal matrix with equal positive real elements, and is a consequence of the conservation of energy (Refs. 4,8). More general conditions will be worked out in the future.

With the interaction (scattering) supermatrix given in Equation 3.2, Equation 3.8 becomes

$$\max\{|\tilde{V}_5|;|\tilde{V}_6|\} \leq \sqrt{|\tilde{V}_5|^2 + |\tilde{V}_6|^2} \leq \frac{|\tilde{S}_{5,3}|}{1 - \max\{|\tilde{S}_{5,6}|;|\tilde{S}_{6,5}|\}} \cdot \tag{3.9}$$
$$\cdot \frac{\sqrt{|[\tilde{S}_1]_{3,1}|^2 + |[\tilde{S}_2]_{3,1}|^2}}{1 - \max\{|\tilde{S}_{3,4}|;|\tilde{S}_{4,3}|\}} \cdot$$
$$\cdot \frac{\max\{|[\tilde{S}_{11}]_{1,2}|;|[\tilde{S}_{22}]_{1,2}|;|[\tilde{S}_{11}]_{2,1}|;|[\tilde{S}_{22}]_{2,1}|\}}{1 - \max\{|[\tilde{S}_{11}]_{1,2}|;|[\tilde{S}_{22}]_{1,2}|;|[\tilde{S}_{11}]_{2,1}|;|[\tilde{S}_{22}]_{2,1}|\}} \cdot \| \left((\tilde{V}_{s_n})_u\right)_1 \|_2$$

The upperbound given above becomes infinity when any one of the reflection coefficients (i.e., those with $|u-v|=1$) equals ± 1. For this situation alterna-

tive bounding procedures should be employed on $\| (\tilde{I}_{n,m})_{\alpha,\beta})_{\lambda,\lambda}^{-1} \|$ in Equation 3.7. One such procedure is to first perform the matrix inversion before bounding the norm. For the example considered here, this procedure gives

$$\max\{|\tilde{V}_7|;|\tilde{V}_8|\} \le \sqrt{|\tilde{V}_7|^2 + |\tilde{V}_8|^2} \le \frac{2\sqrt{2}|\tilde{S}_{7,5}|}{1-|\tilde{S}_{7,8}|\ |\tilde{S}_{8,7}|} \quad \frac{8\sqrt{|[\tilde{S}_1]_{3,1}|^2 + |[\tilde{S}_2]_{3,1}|^2}}{1-|\tilde{S}_{3,4}|\ |\tilde{S}_{6,5}|} \tag{3.10}$$

$$\times \frac{4}{1-\max\{|[\tilde{S}_{11}]_{1,2}\ [\tilde{S}_{11}]_{2,1}|;|[\tilde{S}_{22}]_{1,2}\ \ [\tilde{S}_{22}]_{2,1}|\}} \quad \| \left((\tilde{V}_{s_n})_\alpha\right)_1 \|_2$$

In obtaining the above equation, the following relation has also been used (see Reference 8)

$$\| (A_{n,m}) \|_2 \le \sqrt{N}\ \| (A_{n,m}) \|_\infty \tag{3.11}$$

where N is the number of columns of the square matrix $(A_{n,m})$.

Equation 3.10 clearly shows that the most effective approach to reduce the internal signal upperbound is to decrease the transmission coefficients $|[\tilde{S}_1]_{3,1}|$, $|[\tilde{S}_2]_{3,1}|$ and $|\tilde{S}_{7,5}|$. These transmission coefficients and the other reflection coefficients have all been defined in Section II. More specifically,

$|\tilde{S}_{7,5}|$ ≡ transmission coefficient at $S_{2;3}$ due to both wire-to-wire aperture penetration and line penetration ($|\tilde{S}^{(L)}_{7,5}|$)

$$|\tilde{S}_{7,5}| \le |\tilde{S}^{(L)}_{7,5}| + \max\left\{2|\tilde{v}_{s_{3,2}}|;\ 2|\tilde{i}_{s_{3,2}}|\right\} \tag{3.12}$$

$|[\tilde{S}_1]_{3,1}|$, $|[\tilde{S}_2]_{3,1}|$ ≡ transmission coefficients at $S_{1;2}$ due to field-to-wire aperture and line penetrations, and

$$\sqrt{|[\tilde{S}_1]_{3,1}|^2 + |[\tilde{S}_2]_{3,1}|^2} \tag{3.13}$$

$$\le \sqrt{|[\tilde{S}^{(L)}_2]_{3,1}|^2 + \max\left\{4|\tilde{v}^{(f)}_{s_{2,1}}|^2;\ 4|\tilde{i}^{(f)}_{s_{2,1}}|^2\right\}}$$

Here, the subscripts of $\tilde{v}_s$, $\tilde{i}_s$, $\tilde{v}_s^{(f)}$ and $\tilde{i}_s^{(f)}$ are referred to layers (see Equations 2.10 and 2.13).

$|[\tilde{S}_{11}]_{1,2}|$, $|[\tilde{S}_{22}]_{1,2}|$ ≡ reflection coefficients at the termination junction in V_1 (see Figures 2.5 and 2.6) for the "imaginary" field wire and the real wire, respectively.

$|[\tilde{S}_{11}]_{2,1}|$, $|[\tilde{S}_{22}]_{2,1}|$ ≡ reflection coefficients at $S_{1;2}$ for the wires (one real wire and one imaginary wire) in V_1.

$|\tilde{S}_{3,4}|$, $|\tilde{S}_{6,5}|$ ≡ reflection coefficients at $S_{1;2}$ and $S_{2;3}$, respectively, for the wire in V_2.

$|\tilde{S}_{7,8}|$, $|\tilde{S}_{8,7}|$ ≡ reflection coefficients at $S_{2;3}$ and the termination junction for the wire in V_3.

Experimental methods leading to the determination of these shielding coefficients will be discussed in Section IV.

For the discussion of the source vector in Equations 3.9 and 3.10 the wire arrangement in Figures 2.5a and 2.6b will be used. Thus,

$$\| ((\tilde{V}_{s_n})_\alpha)_1 \|_2 = \left\| \begin{pmatrix} a[\tilde{E}_{sc} + Z_o \tilde{H}_{sc}] \\ \tilde{Z}_c \tilde{I}_{sc} \end{pmatrix} \begin{pmatrix} a[-\tilde{E}_{sc} + Z_o \tilde{H}_{sc}] \\ \tilde{Z}_c \tilde{I}_{sc} \end{pmatrix} \right\|_2 \tag{3.14}$$

$$\leq \sqrt{2}\{a^2[|\tilde{E}_{sc}| + Z_o|\tilde{H}_{sc}|]^2 + |\tilde{Z}_c \tilde{I}_{sc}|^2\}^{1/2}$$

where Z_c is the normalization impedance for the real wire. For the imaginary wire one also has,

$$[\tilde{S}_{11}]_{2,1} = -1, \quad [\tilde{S}_{11}]_{1,2} = 0. \tag{3.15}$$

IV. DETERMINATION OF INTERACTION (SCATTERING) SUPERMATRIX ELEMENTS FOR LINE AND APERTURE PENETRATIONS

In Sections II and III, it was concluded that an internal signal upperbound can be estimated once the scattering matrices of the shields, the termination junctions, and the source environment are known. In this section, methods for the determination of the scattering matrix elements will be discussed.

1. SCATTERING MATRIX FOR LINE PENETRATION

The scattering matrix for the line penetration through a shield is defined through the combined voltages via (see Equation 2.2 and Figure 4.1a)

$$\begin{pmatrix} ((\tilde{V}_n^{(+)})_\alpha)_\lambda - ((\tilde{Z}_{c_{n,m}})_\alpha)_\lambda \cdot ((\tilde{I}_n^{(+)})_\alpha)_\lambda \\ ((\tilde{V}_n^{(+)})_\beta)_{\lambda+1} + ((\tilde{Z}_{c_{n,m}})_\beta)_{\lambda+1} \cdot ((\tilde{I}_n^{(+)})_\beta)_{\lambda+1} \end{pmatrix} \equiv$$

$$\begin{pmatrix} ((\tilde{S}_{n,m})_{\alpha',\alpha})_{\lambda,\lambda} ((\tilde{S}_{n,m})_{\alpha',\beta'})_{\lambda,\lambda+1} \\ ((\tilde{S}_{n,m})_{\beta,\alpha})_{\lambda+1,\lambda} ((\tilde{S}_{n,m})_{\beta,\beta'})_{\lambda+1,\lambda+1} \end{pmatrix} \odot \begin{pmatrix} ((\tilde{V}_n^{(+)})_\alpha)_\lambda + ((\tilde{Z}_{c_{n,m}})_\alpha)_\lambda \cdot ((\tilde{I}_n^{(+)})_\alpha)_\lambda \\ ((\tilde{V}_n^{(+)})_\beta)_{\lambda+1} - ((\tilde{Z}_{c_{n,m}})_\beta)_{\lambda+1} ((\tilde{I}_n^{(+)})_\beta)_{\lambda+1} \end{pmatrix} \tag{4.1}$$

where, if one uses the wave indices (see Figure 4.1)

$$\begin{pmatrix} ((\tilde{S}_{n,m})_{\alpha',\alpha})_{\lambda,\lambda} & ((\tilde{S}_{n,m})_{\alpha',\beta'})_{\lambda,\lambda+1} \\ ((\tilde{S}_{n,m})_{\beta,\alpha})_{\lambda+1,\lambda} & ((\tilde{S}_{n,m})_{\beta,\beta'})_{\lambda+1,\lambda+1} \end{pmatrix} \equiv \begin{pmatrix} (\tilde{S}_{n,m})_{u+1,u} & (\tilde{S}_{n,m})_{u+1,v+1} \\ (\tilde{S}_{n,m})_{v,u} & (\tilde{S}_{n,m})_{v,v+1} \end{pmatrix}$$

The definition of the combined voltages clearly requires the knowledge of the characteristic impedance matrix ($\tilde{Z}_{c_{n,m}}$) of the wires. For a multiwire

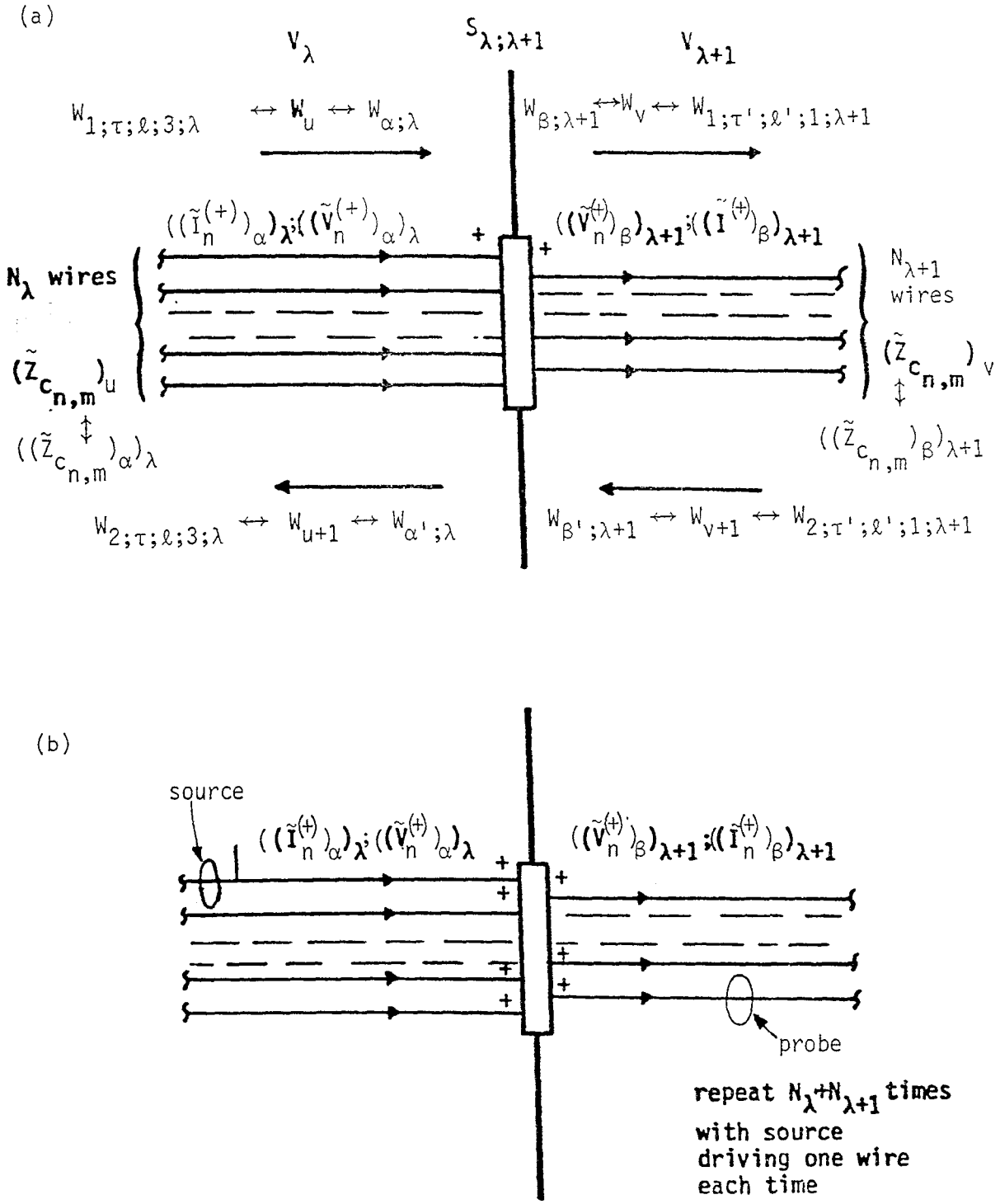

Figure 4.1. (a) Schematic drawing of a wire bundle penetrating through a shield, and (b) experimental setup to estimate the associated scattering matrix.

case, the determination of ($\tilde{Z}_{c_{n,m}}$) might be difficult, if not impossible. However, at this moment, the assumption that ($\tilde{Z}_{c_{n,m}}$) is known will be made.

From Equation 4.1, one can see that there are $(N_\lambda + N_{\lambda+1})^2$ scattering matrix coefficients to be determined if there are N_λ and $N_{\lambda+1}$ wires, respectively. If certain voltage and/or current sources are applied to the wire systems and voltage and current responses are measured on all the wires, then $(N_\lambda + N_{\lambda+1})$ equations can be obtained for the scattering matrix coefficients. That is to say, in order to completely determine the scattering matrix, one needs to perform $(N_\lambda + N_{\lambda+1})$ independent such tests. One way to accomplish this is to apply the source to one wire for each test (see Figure 4.1b). The number of independent experiments can be reduced, if one has certain a priori knowledge about the shields. For example, if the shield is symmetric and satisfies reciprocity, the required experiments can be cut by one-half.

The above description is for the multiwire case. In the case that there is only one wire on each side, Equation 4.1 takes the following form (see Figure 4.1a)

$$\begin{pmatrix} \tilde{V}^{(+)}_{\alpha\,;\,\lambda} - \tilde{Z}_{c_{\alpha\,;\,\lambda}} & \tilde{I}^{(+)}_{\alpha\,;\,\lambda} \\ \tilde{V}^{(+)}_{\beta\,;\,\lambda+1} + \tilde{Z}_{c_{\beta\,;\,\lambda+1}} & \tilde{I}^{(+)}_{\beta\,;\,\lambda+1} \end{pmatrix} \equiv \tag{4.2}$$

$$\begin{pmatrix} \tilde{S}_{\alpha',\alpha\,;\,\lambda,\lambda} & \tilde{S}_{\alpha',\beta';\lambda,\lambda+1} \\ \tilde{S}_{\beta,\alpha;\lambda+1,\lambda} & \tilde{S}_{\beta,\beta';\lambda+1,\lambda+1} \end{pmatrix} \cdot \begin{pmatrix} \tilde{V}^{(+)}_{\alpha\,;\,\lambda} + \tilde{Z}_{c_{\alpha\,;\,\lambda}} & \tilde{I}^{(+)}_{\alpha\,;\,\lambda} \\ \tilde{V}^{(+)}_{\beta\,;\,\lambda+1} - \tilde{Z}_{c_{\beta\,;\,\lambda+1}} & \tilde{I}^{(+)}_{\beta\,;\,\lambda+1} \end{pmatrix}$$

where, if one uses the wave indices,

$$\begin{pmatrix} \tilde{S}_{\alpha',\alpha\,;\,\lambda,\lambda} & \tilde{S}_{\alpha',\beta';\lambda,\lambda+1} \\ \tilde{S}_{\beta,\alpha;\lambda+1,\lambda} & \tilde{S}_{\beta,\beta';\lambda+1,\lambda+1} \end{pmatrix} \equiv \begin{pmatrix} \tilde{S}_{u+1,u} & \tilde{S}_{u+1,v+1} \\ \tilde{S}_{v,u} & \tilde{S}_{v,v+1} \end{pmatrix}$$

The scattering matrix can be determined from the experiments shown in Fig. 4.2a and solving a set of linear algebraic equations. In the case that the wires can be disconnected, the process of solving the linear equations can be avoided by performing a somewhat different experiment. Such experiments are shown in Figure 4 2b. From the experiment in Figure 4 2b, one immediately has

$$\tilde{S}_{u+1,u} = \tilde{S}_{\alpha',\alpha;\lambda,\lambda} = \left.\frac{\tilde{V}^{(+)}_{\alpha\,;\,\lambda} - \tilde{Z}_{c_{\alpha\,;\,\lambda}}\,\tilde{I}^{(+)}_{\alpha\,;\,\lambda}}{\tilde{V}^{(+)}_{\alpha\,;\,\lambda} + \tilde{Z}_{c_{\alpha\,;\,\lambda}}\,\tilde{I}^{(+)}_{\alpha\,;\,\lambda}}\right|_{\tilde{V}^{(+)}_{\beta\,;\,\lambda+1} - \tilde{Z}_{c_{\beta;\lambda+1}}\tilde{I}^{(+)}_{\beta\,;\lambda+1}=0} \tag{4.3}$$

$$\tilde{S}_{v,u} = \tilde{S}_{\beta,\alpha;\lambda+1,\lambda} = \left.\frac{\tilde{V}^{(+)}_{\beta\,;\,\lambda+1} + \tilde{Z}_{c_{\beta\,;\,\lambda+1}}\,\tilde{I}^{(+)}_{\beta\,;\,\lambda+1}}{\tilde{V}^{(+)}_{\alpha\,;\,\lambda} + \tilde{Z}_{c_{\alpha\,;\,\lambda}}\,\tilde{I}^{(+)}_{\alpha\,;\,\lambda}}\right|_{\tilde{V}^{(+)}_{\beta\,;\,\lambda+1} - \tilde{Z}_{c_{\beta\,;\,\lambda+1}}\,\tilde{I}^{(+)}_{\beta\,;\,\lambda+1}=0}$$

and from the experiment in Figure 4.2c,

$$\tilde{S}_{u+1,v+1} = \tilde{S}_{\alpha',\beta';\lambda,\lambda+1} = \left.\frac{\tilde{V}^{(+)}_{\alpha\,;\,\lambda} - \tilde{Z}_{c_{\alpha\,;\,\lambda}}\,\tilde{I}^{(+)}_{\alpha\,;\,\lambda}}{\tilde{V}^{(+)}_{\beta\,;\,\lambda+1} - \tilde{Z}_{c_{\beta;\lambda+1}}\,\tilde{I}^{(+)}_{\beta\,;\,\lambda+1}}\right|_{\tilde{V}^{(+)}_{\alpha\,;\,\lambda} + \tilde{Z}_{c_{\alpha;\lambda}}\,\tilde{I}^{(+)}_{\alpha;\,\lambda}=0}$$

$$\tilde{S}_{v,v+1} = \tilde{S}_{\beta,\beta';\lambda+1,\lambda+1} = \left.\frac{\tilde{V}^{(+)}_{\beta\,;\,\lambda+1} + \tilde{Z}_{c_{\beta;\lambda+1}}\,\tilde{I}^{(+)}_{\beta\,;\,\lambda+1}}{\tilde{V}^{(+)}_{\beta\,;\,\lambda+1} - \tilde{Z}_{c_{\beta;\lambda+1}}\,\tilde{I}^{(+)}_{\beta\,;\,\lambda+1}}\right|_{\tilde{V}^{(+)}_{\alpha\,;\,\lambda} + \tilde{Z}_{c_{\alpha;\lambda}}\,\tilde{I}^{(+)}_{\alpha\,;\,\lambda}=0} \tag{4.4}$$

These experimental setups of Figures 4.2b and 4.2c can also be extended to multiwire cases.

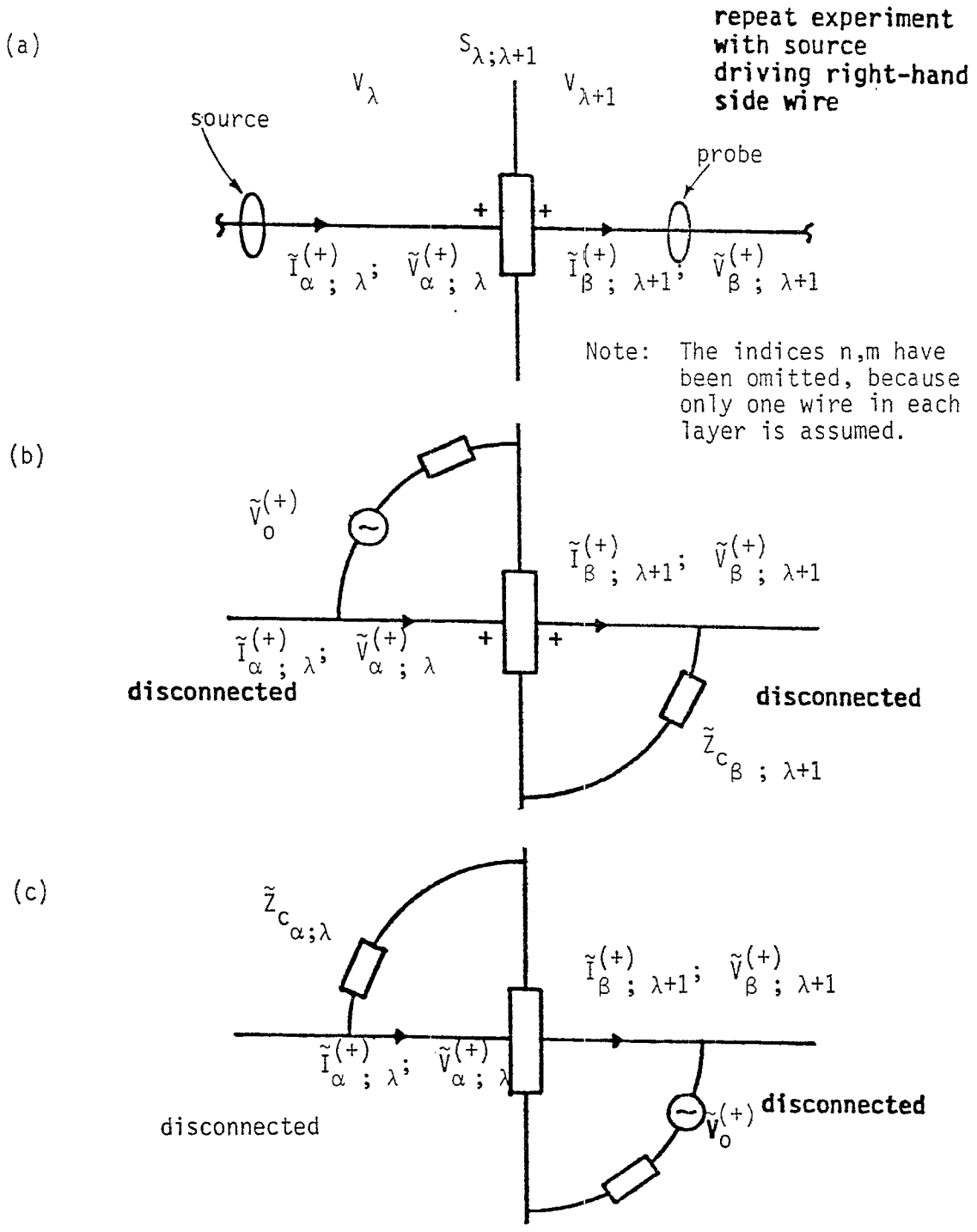

Figure 4.2. (a) Schematic drawing of the experimental setup for the estimate of the scattering matrix for the single wire line penetration; (b) & (c) an alternative version of (a) when the wires can be disconnected.

2. SCATTERING (REFLECTION) MATRIX FOR TERMINATION JUNCTION

A termination junction can be considered as a shield which does not allow signal penetrating into the next layer. The discussion in Part 1 of this section is thus applicable to a junction. In this case, one will simply have, instead of Equation 4.1 (see Figure 4.3).

$$((\tilde{V}_n^{(+)})_\alpha)_\lambda - ((\tilde{Z}_{c_{n,m}})_\alpha)_\lambda \cdot ((\tilde{I}_n^{(+)})_\alpha)_\lambda \tag{4.5}$$

$$\equiv ((\tilde{S}_{n,m})_{\alpha',\alpha})_{\lambda,\lambda} \cdot \left[((\tilde{V}_n^{(+)})_\alpha)_\lambda + ((\tilde{Z}_{c_{n,m}})_\alpha)_\lambda \cdot ((\tilde{I}_n^{(+)})_\alpha)_\lambda \right]$$

where, if the wave indices are used,

$$((\tilde{S}_{n,m})_{\alpha',\alpha})_{\lambda,\lambda} \equiv (\tilde{S}_{n,m})_{u+1,u}$$

The reflection matrix can be determined by performing experiments similar to those of Figures 4.1 and 4.2, with the wires in the $(\lambda+1)$ layer discarded.

When the loading impedance is known, this reflection matrix can also be calculated analytically

$$(\tilde{S}_{n,m})_{u+1,u} \equiv ((\tilde{S}_{n,m})_{\alpha',\alpha})_{\lambda,\lambda} \tag{4.6}$$

$$= \left[(\tilde{Z}_{L_{n,m}}) + ((\tilde{Z}_{c_{n,m}})_\alpha)_\lambda \right]^{-1} \cdot \left[(\tilde{Z}_{L_{n,m}}) - ((\tilde{Z}_{c_{n,m}})_\alpha)_\lambda \right]$$

This equation is particularly useful for the estimate of the reflection matrix elements associated with small antennas at the outermost layer where the input impedances $(\tilde{Z}_{L_{n,m}})$ of the antennas are known.

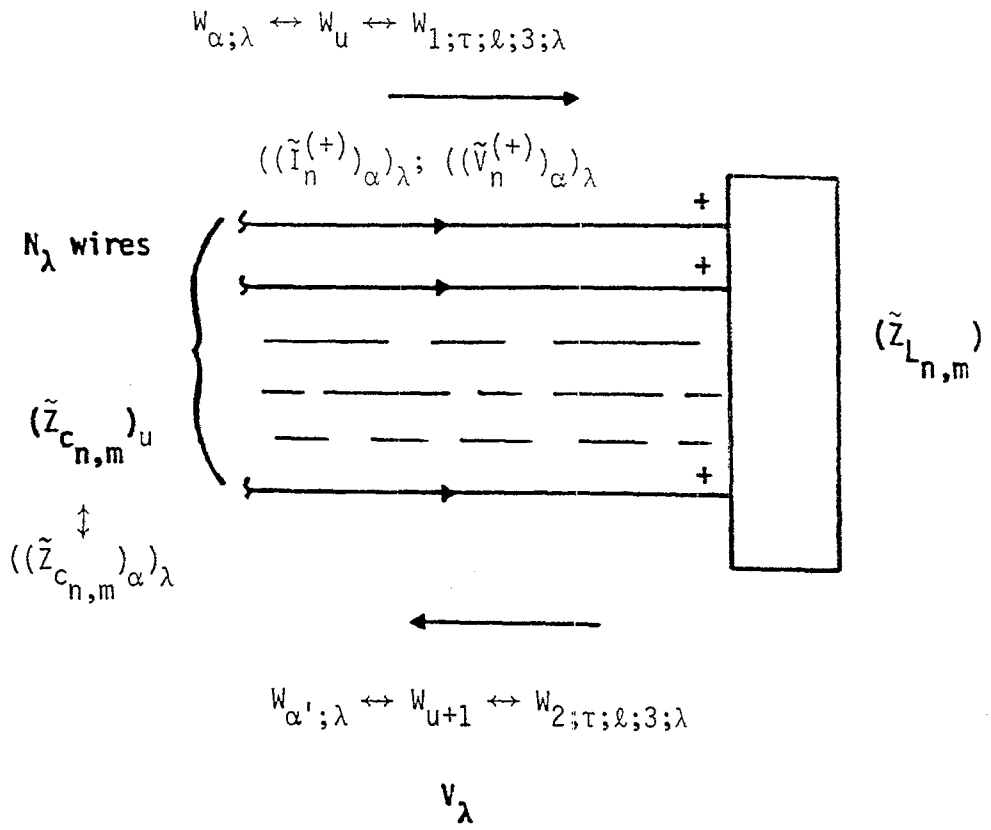

Figure 4.3. Schematic drawing of a terminating junction.

3. SCATTERING MATRIX FOR WIRE-TO-WIRE APERTURE PENETRATIONS

When the shield of Figure 4.1a has apertures the scattering supermatrix derived for the line penetration has to be modified. From the consideration of Section II, it was shown that only the off-diagonal blocks need modification, namely, the transmission matrices. For upperbound estimates one only needs two experimental setups for each aperture to determine the maximum $|\tilde{V}^{(+)}_{s_{\lambda+1}}/\tilde{I}^{(+)}_{\alpha;\lambda}|$ and $|\tilde{I}^{(+)}_{s_{\lambda+1}}/\tilde{V}^{(+)}_{\alpha;\lambda}|$ (see Equation 2.10). The results from these experiments can then be used for all the scattering matrix elements associated with wires interacting through an aperture.

The experiments shown in Figure 4.4 can be performed by using wires not associated with the system, thereby avoiding the necessity of shorting and/or disconnecting the wires in the system. The experiments are also arranged with the wires immediately outside the exclusion regions to obtain the maximum allowable interaction. The exclusion regions should be at least one maximum aperture linear dimension away from the aperture. The effect of the aperture on the current and voltage on the excitation wire can be neglected.

Using the experimental results thus obtained, one can calculate the upperbounds of the scattering matrix elements according to Equation 2.11.

The quantities $|\tilde{V}^{(+)}_{s_{\lambda+1}}/\tilde{I}^{(+)}_{\alpha;\lambda}|$ and $|\tilde{I}^{(+)}_{s_{\lambda+1}}/\tilde{V}^{(+)}_{\alpha;\lambda}|$ can also be analytically estimated, provided that the maximum electric (α_e) and magnetic (α_m) polarizabilities and known. In Figure 4.4, if the exclusion regions are hemispheres (with radius R of the exclusion region > maximum linear aperture dimension), these quantities are approximately (Reference 9),

$$|\tilde{I}^{(+)}_{s_{\lambda+1}} / \tilde{V}^{(+)}_{\alpha\,;\,\lambda}| \simeq \left| \frac{2s\varepsilon_o}{R^2} \quad \frac{\alpha_e}{\ell n[2R/r_o]} \right| \tag{4.7}$$

$$|\tilde{V}^{(+)}_{s_{\lambda+1}} / \tilde{I}^{(+)}_{\alpha\,;\,\lambda}| \simeq \left| \frac{s\mu_o}{2\pi R^2} \quad \alpha_m \right|$$

where r_o is the radius of the wire in the $(\lambda+1)$-layer in the experimental setup and should be greater than those of the wires in the actual system involving in the aperture interaction process. An alternative analytical

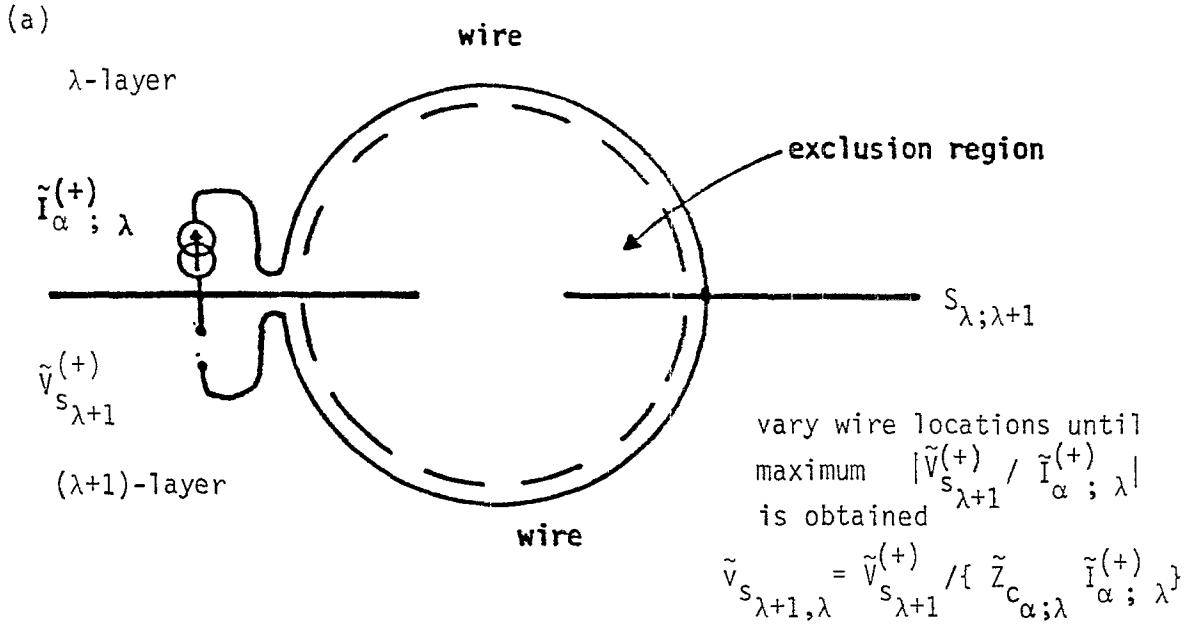

Note: The indices n,m have been omitted, because only one wire in each layer is assumed.

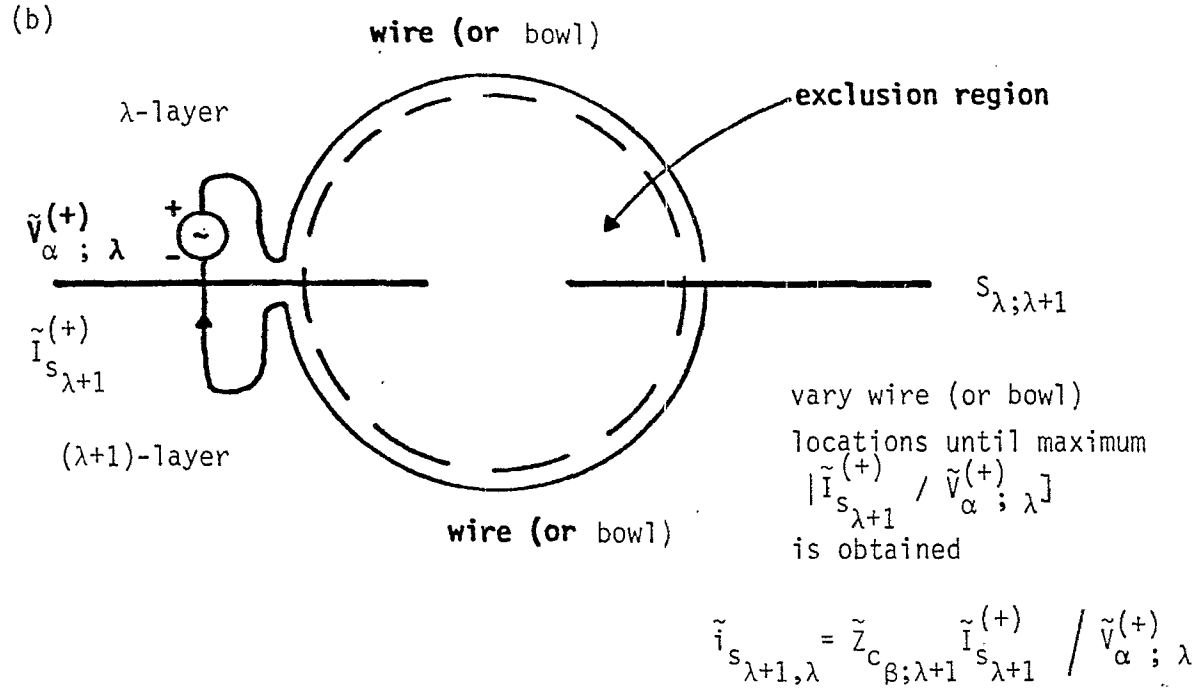

Figure 4.4. Experimental setups for the estimate of the scattering matrix elements associated with the wires involved in the wire-to-wire (a) magnetic field, and (b) electric field aperture penetrations.

estimate can also be obtained based on the maximum electric and magnetic fluxes penetrating an aperture. The estimate is given by

$$|\tilde{I}^{(+)}_{s_{\lambda+1}} \; / \; \tilde{V}^{(+)}_{\alpha} \; ; \lambda| \simeq |s \; \varepsilon_o \; A/R \;| \qquad (4.8)$$

$$|\tilde{V}^{(+)}_{s_{\lambda+1}} \; / \; \tilde{I}^{(+)}_{\alpha} \; ; \lambda| \simeq |s\mu_o \; A_m/[2R]|$$

where A is the area of the aperture and A_m is the maximum magnetic flux ($\tilde{\Phi}_m$) penetration factor defined via $A_m = \tilde{\Phi}_m/(\mu_o \tilde{H}_{sc})$ (for a circular aperature with radius = R/2, $A_m = R^2/4$). The first equation in Equation 4.8 can be used as the approximate result for the case when bowls are used in the electric field interaction experiment.

4. SCATTERING MATRIX FOR FIELD-TO-WIRE APERTURE PENETRATIONS

In Section II, it was shown that the field-to-wire interaction through an aperture (which is important only in the outermost shield) can be treated by introducing an additional imaginary wire in the outer layer. Because of the introduction of this wire, additional scattering matrix elements have to be included. The upperbound of the additional scattering matrix elements can be estimated by Equation 2.13.

Equation 2.13 is similar to Equation 2.10. Most arguments raised in Part 3 of this section are thus applicable here. The experiment setups in Figure 4.5 can be used for the determination of the upperbound estimates of $|\tilde{S}_{\beta,\alpha;2,1}|$ in Equation 2.13. The sources required in the experiments are uniform electric and/or magnetic fields near the aperture when the aperture is covered with conductor. This can be accomplished by performing the experiments in a special FINES simulator (see Reference 10).

Formulas similar to Equations 4.7 and 4.8 can be obtained for this type of interaction as, with a = R,

$$|\,[\tilde{I}^{(f)}_s]_2 \; / \; [R\,\tilde{E}_{sc}]\,| \simeq \left| \frac{2 \; s\varepsilon_o \alpha_e}{R^2 \ell n[2R/r_o]} \right|$$

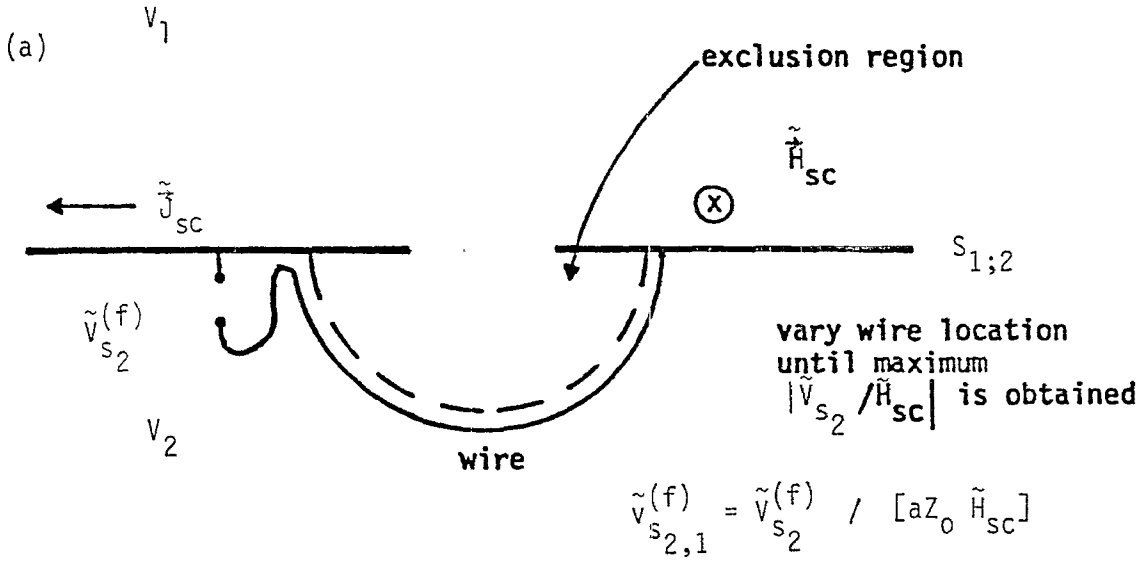

Note: The indices n,m have been omitted because there is only one wire in V_2.

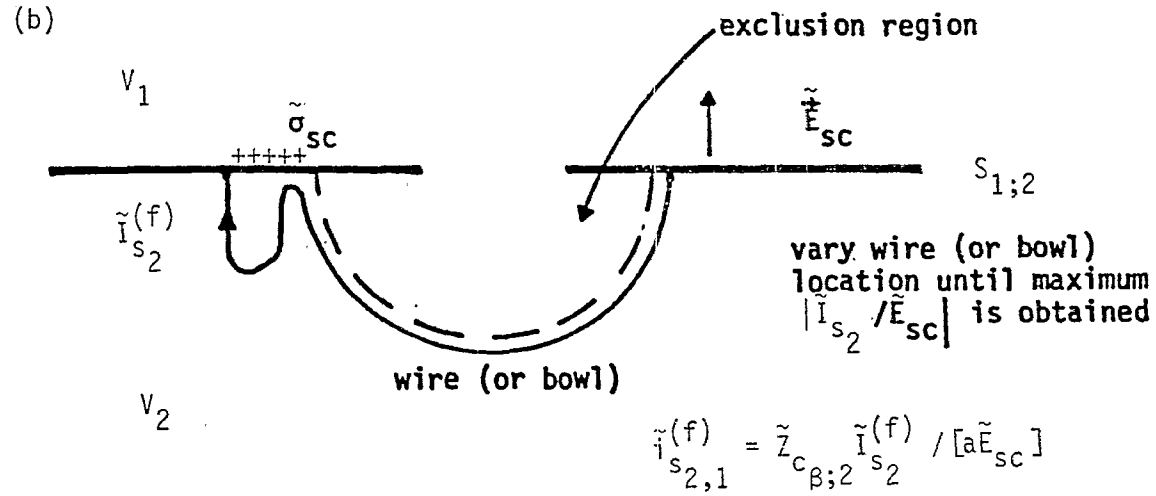

Figure 4.5. Experimental setups for the estimate of the scattering matrix elements associated with the wires involved in the field-to-wire (a) magnetic field, and, (b) electric field aperture penetrations.

$$\left| \tilde{V}_{s_2}^{(f)} \;/\; [R\, Z_o \tilde{H}_{sc}] \right| \simeq \left| \frac{s\mu_o \alpha_m}{Z_o \pi R^2} \right| \qquad (4.9)$$

and

$$\left| \tilde{I}_{s_2}^{(f)} \;/\; [R\, \tilde{E}_{sc}] \right| \simeq \left| s\, \varepsilon_o\, A/R \right|$$

$$\left| \tilde{V}_{s_2}^{(f)} \;/\; [R\, Z_o \tilde{H}_{sc}] \right| \simeq \left| s\, \mu_o\, A_m \,/\, [R\, Z_o] \right| \qquad (4.10)$$

In the discussion of Parts 3 and 4 of this section, possible resonances of the cavity formed by two adjacent shields are neglected (i.e., shield-to-shield interaction for the field is neglected). One way to include the resonance effect is to perform the experiments with both shields present.

V. USE OF EXPERIMENTAL RESULTS IN SHIELD DESIGN PROCEDURES

Having related the signal responses to the electromagnetic sources in terms of norms of shield scattering matrices and having established methods to estimate these norms, one can then use the process to analyze and synthesize (or design) shields in a system. Here, only the design (or, synthesis) aspect will be addressed.

There are two kinds of system shielding design one may encounter. One is for a system still on the drawing board, and the other is for an existing system requiring shielding improvement (i.e., hardening). For an existing system, one might not have the freedom of changing the layer configuration and the only possibility of hardening the system may be to alter the shield characteristics by implementing hardening fixes at the shields. This section will address how the results of previous sections can be used in the shielding design for an existing system. The discussion will also be useful in the shielding design of a new system.

1. GENERAL PROCEDURE

In Reference 1, a shielding design procedure has been laid down. The procedure is duplicated below with minor modifications and additions.

a. Consider some elementary topology defined to at least sublayer level (e.g., Figure 2.1)

b. Identify the sources in each sublayer corresponding to electromagnetic environments of interest.

c. Identify the allowable maximum signal levels in each sublayer of concern associated with each electromagnetic environment.

d. Identify the paths P_n associated with each pair of source sublayers (b) and response sublayer (c) of concern.

e. Allocate "shielding"along each path P_n such that the sources (b) produce no more response than allowed in sublayers (c).

f. Partition the shielding along each P_n among the corresponding subshields encountered on P_n. This gives maximum allowable values to the norms of each corresponding subshield transmission and reflection matrices.

g. For each subshield consider all paths P_n that pass through it. Choose the tranmission and reflection matrix norms to be the least values of those concern for all P_n in (f).

h. Perform experiments to select subshield hardening approaches satisfying the transmission and reflection matrix norm requirements established in (g).

i. Write specifications for subshield hardening requirements.

2. EXAMPLE

To demonstrate how to use the above shielding design procedure, consider the example of Section III. For simplicity, each subshield in the example is assumed to have only one line and one aperture penetration. The relationship between the sources and responses is then given in Equation 3.10. The shielding design procedure proceeds as follows

a. The topological and interaction sequence diagrams are shown in Figure 3.1.

b. The sources (EMP, lightning, etc.) exist only in V_1, and are assumed to be not greater than 10^4 V, i.e.,

$$\| ((\tilde{V}_{s_n})_\alpha)_1 \|_2 \leq \sqrt{2} \left\{ a^2 \left[|\tilde{E}_{sc}| + Z_o |\tilde{H}_{sc}| \right]^2 + |\tilde{Z}_c \tilde{I}_{sc}|^2 \right\}^{\frac{1}{2}}$$

$$\leq 10^4 \text{ (Volts)} \qquad (5.1)$$

c. The signal responses of concern are in V_3. The maximum allowable combined voltage is assumed to be 100 mV, i.e.,

$$\left\| \begin{pmatrix} \tilde{V}_7 \\ \tilde{V}_8 \end{pmatrix} \right\| \leq 100 \text{ (mV)} \qquad (5.2)$$

d. There is only one path (Each shield along the path has two penetrations).

e. From Steps b and c, the shields along the path must reduce the signal levels by at least 5 orders of magnitude ($10^4 \rightarrow 10^{-1}$, 100 dB).

f. There are various ways to satisfy the overall shielding requirement established in Step e. Take $|[\tilde{S}_{22}]_{1,2}| = 0.5$ in Equation 3.10 which is determined mainly by the structure of the protrude wire (or antenna), and $|\tilde{S}_{8,7}| \leq 1$ which is determined by the loading impedance. Then, one possible way to satisfy the overall shielding requirement is to have

$$|[\tilde{S}_{22}]_{2,1}| < 1$$

$$|\tilde{S}_{3,4}| \simeq |\tilde{S}_{6,5}| \simeq |\tilde{S}_{7,8}| \leq 0.9$$

$$|\tilde{S}_{7,5}| \leq |\tilde{S}_{7,5}^{(L)}| + \max\left\{2|\tilde{v}_{s_{3,2}}|;\ 2|\tilde{i}_{s_{3,2}}|\right\} \leq 2\times10^{-5}$$

$$\sqrt{|[\tilde{S}_1]_{3,1}|^2 + |[\tilde{S}_2]_{3,1}|^2}$$

$$\leq \sqrt{|[\tilde{S}_2^{(L)}]_{3,1}|^2 + \max\left\{4|\tilde{v}_{s_{2,1}}^{(f)}|^2;\ 4|\tilde{i}_{s_{2,1}}^{(f)}|^2\right\}} \leq 10^{-4} \qquad (5.3)$$

It should be emphasized that, except $\tilde{v}_s$, $\tilde{i}_s$, $\tilde{v}_s^{(f)}$ and $\tilde{i}_s^{(f)}$ where indices are referred to layers, all the outermost indices for the variables are referred to waves. If it turns out this set of values is difficult to achieve with available hardening fixes, other sets of values may work.

g. This step should be skipped, since there is only one path.

h. Perform experiments with various hardening fixes (such as, filters, arrestors along the wires, and wire meshes at the aperture) to select the ones satisfying the requirements established in Step f.

i. Write specifications for the proven hardening approach.

VI. FUTURE DEVELOPMENT

The bounding methodology presented here suffers from several restrictive features and thus leaves ground for improvement. This leads to the following suggestions for future developments.

1. OPTIMIZATION OF NORMALIZATION IMPEDANCES

The normalization impedances are required in the definition of the combined voltages which in turn are the basic quantities in the discussion. For the internal wires, the natural quantities to use for the normalization impedances are their characteristic impedances. These characteristic impedances contain the information about how the wires interact among themselves. For a complicated system, the determination of the characteristic impedances could be nearly impossible. On the other hand, for the external wires in V_1 the use of the normalization impedances to construct the combined voltages is completely artificial. If too large or too small a normalization impedance is used, the norm will give an inaccurate conclusion (for example, if $\tilde{Z}_c$ is infinitely large for the source vector of Equation 3.14, then the source vector information for the field coupling through the aperture will be lost).

For the above reasons, one inevitable question would be "what are the optimal normalization impedances one should use to make the bounding methodology simple and accurate?" For an order-of-magnitude estimate, the use of a diagonal normalization matrix with the diagonal elements in the order of 100Ω could be a reasonable choice. However, its validity or the choice of other values so that a tighter bound can be obtained requires further considerations.

2. OPTIMATION OF LENGTH PARAMETER IN CHARACTERIZATION OF FIELD APERTURE PENETRATION

In Section II, it was seen that the length parameter "a" is required in the definition of combined voltages for the field-to-wire interaction through an aperture. This length parameter is artificial. In the case where there is only aperture interaction through the outermost shield, the use of an

arbitrary "a" should be acceptable. On the other hand, in the case where the shield allows both line and aperture penetrations, an inadequate "a" value might give an inaccurate emphasis on the aperture penetration. A reasonable value for this length parameter might be the linear dimension of the aperture. This conjecture requires further consideration.

3. LAYER(SUBLAYER)-LAYER(SUBLAYER) INTERACTION

The zero-tube-length approximation has been used to simplify the scattering matrix formulation. By doing so, the layer-layer interaction and the propagation behavior between layers are excluded from the formulation. The exclusion might result in loose upperbound estimates and inaccurate resonant phenomena. The formulation to include the layer-layer interaction and the propagation behavior between layers requires further consideration.

4. DIFFUSION PENETRATION

When the part of a shield that allows for diffusion penetration covers only an electrically small region, the diffusion penetration can be treated as an aperture penetration. When the region is electrically large, an alternative approach needs to be sought.

5. TIME-DOMAIN CONSIDERATION

The signal bounding has been discussed in the complex frequency domain, or for CW signals. For a transient electromagnetic interference such as EMP or lightning, the time-domain consideration is also needed. In principle, it can be obtained from the frequency-domain consideration. For example, in the time-domain the matrices in Equations 2.6 and 2.7 resulting from the good shielding approximation will become convolution operators. For a more general case, there may be even nonlinear time-domain operators.

REFERENCES

1. Baum, C.E., "Electromagnetic Topology: A Formal Approach to the Analysis and Design of Complex Electronic Systems," Interaction Notes, Note 400, Air Force Weapons Laboratory, Kirtland Air Force Base, New Mexico, September 1980.

2. Vance, E.F., W. Graf, J.E. Nanevicz, "Unification of Electromagnetic Specifications and Standards, Part I. Evaluation of Existing Practices," Interaction Notes, Note 420, Air Force Weapons Laboratory, Kirtland Air For Base, New Mexico, July 1981.

3. Baum, C.E., T.K. Liu, F.M. Tesche, "On the Analysis of General Multiconductor Transmission-Line Networks," Interaction Notes, Note 350, Air Force Weapons Laboratory, Kirtland Air Force Base, New Mexico, November 1979.

4. Baum, C.E., "Norms and Eigenvector Norms, "Mathematics Notes, Note 63, Air Force Weapons Laboratory, Kirtland Air Force Base, New Mexico, November 1979.

5. P. Lancaster, Theory of Matrices, Academic Press, 1969.

6. Baum, C.E., "Sublayer Sets and Relative Shielding Order in Electromagnetic Topology," Interaction Notes, Note 416, Air Force Weapons Laboratory, Kirtland Air Force Base, New Nexico, April 1982.

7. Baum, C.E., "Black Box Bounds," to be published as an Interaction Note.

8. Agrawal, A.K., C.E. Baum, "Bounding of Signal Levels at Terminations of a Multiconductor Transmission-Line Network," Interaction Notes, Note 419, Air Force Weapons Laboratory, Kirtland Air Force Base, New Mexico, April 1983.

9. Lee, K.S.H., editor, "EMP Interaction: Principles, Techniques and Reference Data," EMP Interaction 2-1, Air Force Weapons Laboratory, Kirtland Air Force Base, New Mexico, December 1980.

10. Baum, C.E., "EMP Simulators for Various Types of Nuclear EMP Environments: An Interim Categorization," IEEE Transactions on Antennas and Propagation, Vol. AP-26,No.1, January 1978. Also, Sensor and Simulation Notes, Note 240, Air Force Weapons Laboratory, Kirtland AFB, New Mexico.

11. Ramo, S., J.R. Whinnery, and T. Van Suzer, Fields and Waves in Communication Electronics, John Wiley and Sons, Inc., New York, 1965.

APPENDIX A

DERIVATION OF SUPERMATRIX EQUATION

An aeronautic system can be described by a topological diagram which can in turn be used to construct a corresponding interaction sequence diagram (see Figure 2.1). An interaction sequence diagram consists of vertices and edges. The vertices represent surfaces and layers (volumes) in the topological diagram, and the edges indicate how the electromagnetic signals transport. On the edges, there are voltages and currents which satisfy the familiar transmission-line equations. The voltages and currents are coupled in the transmission-line equations. This complexity can be avoided by introducing the following combined voltages (see Figure A.1a),

$$(\tilde{V}_n)_u = (\tilde{V}_n^{(+)})_u + (\tilde{Z}_{c_{n,m}})_u \cdot (\tilde{I}_n^{(+)})_u$$

$$(\tilde{V}_n)_v = (\tilde{V}_n^{(+)})_u - (\tilde{Z}_{c_{n,m}})_u \cdot (\tilde{I}^{(+)})_u \qquad \text{(A.1)}$$

With the combined voltages as the dependent variables, the transmission-line equations become uncoupled and are given as

$$\frac{d}{dz_u}(\tilde{V}_n)_u = -(\tilde{\gamma}_{c_{n,m}})_u \cdot (\tilde{V}_n)_u + (\tilde{V}'_{s_n})_u^{temp}$$

$$\frac{d}{dz_u}(\tilde{V}_n)_v = (\tilde{\gamma}_{c_{n,m}})_u \cdot (\tilde{V}_n)_v + (\tilde{V}'_{s_n})_v^{temp} \qquad \text{(A.2)}$$

where $(\tilde{\gamma}_{c_{n,m}})_u$ is the propagation matrix, $(\tilde{V}'_{s_n})_u^{temp}$ and $(\tilde{V}'_{s_n})_v^{temp}$ are distributed combined voltage source vectors given by (see Figure A.1b)

$$(\tilde{V}'_{s_n})_u^{temp} = (\tilde{V}_{s_n}^{(+)'})_u + (\tilde{Z}_{c_{n,m}})_u \cdot (\tilde{I}_{s_n}^{(+)'})_u$$

(a)

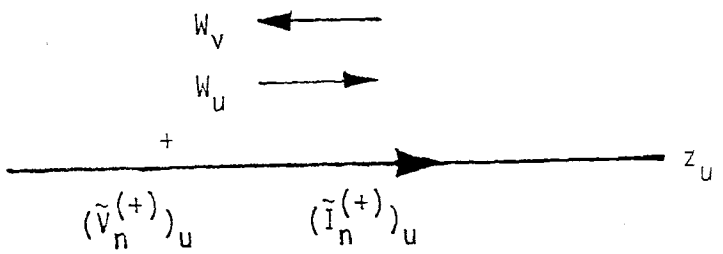

$$(\tilde{V}_n)_u = (\tilde{V}_n^{(+)})_u + (\tilde{Z}_{c_{n,m}})_u \cdot (\tilde{I}_n^{(+)})_u$$

$$(\tilde{V}_n)_v = (\tilde{V}_n^{(+)})_u - (\tilde{Z}_{c_{n,m}})_u \cdot (\tilde{I}_n^{(+)})_u$$

(b)

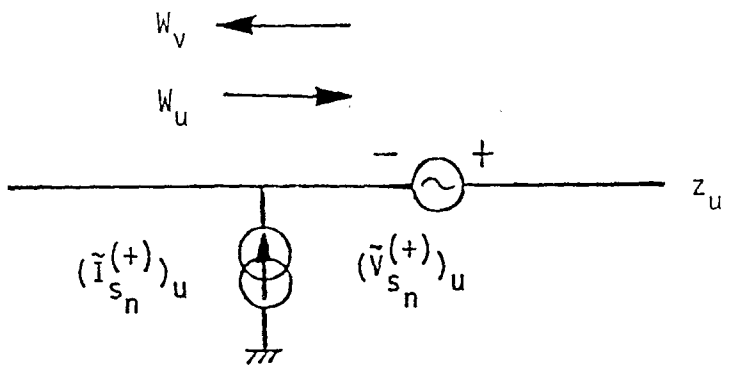

$$(\tilde{V}_{s_n})_u^{temp} = (\tilde{V}_{s_n}^{(+)})_u + (\tilde{Z}_{c_{n,m}})_u \cdot (\tilde{I}_{s_n}^{(+)})_u$$

$$(\tilde{V}_{s_n})_v^{temp} = (\tilde{V}_{s_n}^{(+)})_u - (\tilde{Z}_{c_{n,m}})_u \quad (\tilde{I}_{s_n}^{(+)})_u$$

$$(\tilde{Z}_{c_{n,m}})_u = (\tilde{Z}_{c_{n,m}})_v$$

Figure A.1. Sign conventions for the real voltages and currents used for (a) the combined voltage definition, and (b) a temporary combined source voltage definition.

$$(\tilde{V}'_{s_n})_v^{temp} = (\tilde{V}^{(+)'}_{s_n})_u - (\tilde{Z}_{c_{n,m}})_u \cdot (\tilde{I}^{(+)'}_{s_n})_u \qquad (A.3)$$

The superscript "temp" is to indicate these are temporary definitions and a different combined voltage source vector will be defined later. Equation A.2, clearly, indicates that the combined voltages of the two oppositively propagating waves still satisfy different differential equations. To unify these two equations, one introduces another coordinate system $z_v = \ell_u - z_u$ for the second equation of Equation A.2 (see Figure A.2a). With this new set of coordinate systems which has $z = 0$ and $z = \ell_u$ (z can be either z_u or z_v, and ℓ_u is the length of the edge) indicating respectively, the initiating and terminating points of the wave, Equation A.2 becomes

$$\frac{d}{dz_u}(\tilde{V}_n)_u = -(\tilde{\gamma}_{c_{n,m}})_u \cdot (\tilde{V}_n)_u + (\tilde{V}'_{s_n})_u \qquad (A.4)$$

Here "u" represents <u>either</u> wave on the edge and

$$(\tilde{V}'_{s_n}) = (\tilde{V}^{(+)'}_{s_n})_u + (\tilde{Z}_{c_{n,m}})_u \cdot (\tilde{I}^{(+)'}_{s_n})_u \qquad (A.5)$$

with $(\tilde{V}^{(+)'}_{s_n})_u$ being positive when it increases with the wave propagating direction and $(\tilde{I}^{(+)'}_{s_n})_u$ being positive when it flows into the edge (Figure A.2b).

Equation A.4 can be solved to relate the combined voltages at the wave terminating points (at $z_u = \ell_u$) to those at the wave initiating points (at $z_u = 0$). Under the assumption of short edge length (i.e., under the condition that $\|((\tilde{\gamma}_{c_{n,m}})_u)\| \; \|(\ell_u)\| << 1$), the relation is simply

$$((\tilde{V}_n)_u)\Big|_{(z_u)=(\ell_u)} = ((\tilde{V}_n)_u)\Big|_{(z_u)=(0)} + ((\tilde{V}_{s_n})_u) \qquad (A.6)$$

(a)

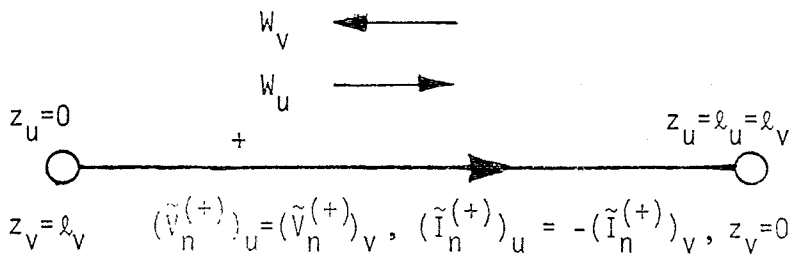

$$(\tilde{V}_n)_u = (\tilde{V}_n^{(+)})_u + (\tilde{Z}_{c_{n,m}})_u \cdot (\tilde{I}_n^{(+)})_u$$

$$(\tilde{V}_n)_v = (\tilde{V}_n^{(+)})_u - (\tilde{Z}_{c_{n,m}})_u \cdot (\tilde{I}_n^{(+)})_u$$

$$= (\tilde{V}_n^{(+)})_v + (\tilde{Z}_{c_{n,m}})_v \cdot (\tilde{I}_n^{(+)})_v$$

(b)

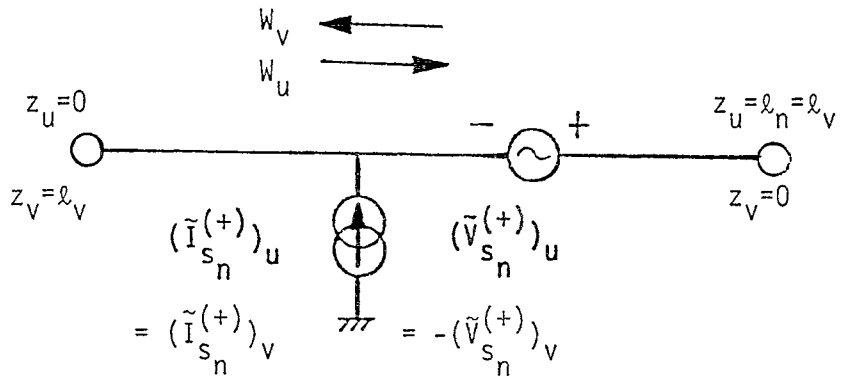

$$(\tilde{V}_{s_n})_u = (\tilde{V}_{s_n}^{(+)})_u + (\tilde{Z}_{c_{n,m}})_u \cdot (\tilde{I}_{s_n}^{(+)})_u$$

$$(\tilde{V}_{s_n})_v = -(\tilde{V}_{s_n}^{(+)})_u + (\tilde{Z}_{c_{n,m}})_u \cdot (\tilde{I}_{s_n}^{(+)})_u$$

$$= (\tilde{V}_{s_n}^{(+)})_v + (\tilde{Z}_{c_{n,m}})_v \cdot (\tilde{I}_{s_n}^{(+)})_v$$

Figure A.2. Sign conventions for the coordinate systems, real voltages and currents used in the definitions of (a) the combined voltages, and (b) the combined source voltage.

where $((\tilde{V}_{s_n})_u)$ is the combined voltage source supervector which is the integral of the corresponding distributed quantity along the edge.

Equation A.6 describes how the combined voltages vary along the edges. One still needs another equation to describe how the combined voltages behave at the vertices. At a vertex, incident waves are scattered. The scattered waves are related to the incident waves through a scattering matrix (see Reference 11). Since the incident and scattered waves at a vertex are, respectively, the terminating and initiating combined voltages on the edges connecting to the vertex, the relationship is given by

$$((\tilde{V}_n)_u)\,|_{(z_u)\,=\,(0)} = ((\tilde{S}_{n,m})_{u,v}) \odot ((\tilde{V}_n)_u)\,|_{(z_u)\,=\,(\ell_u)} \tag{A.7}$$

Equations A.6 and A.7 can then be combined to give

$$\begin{aligned}[[((1_{n,m})_{u,v}) - ((\tilde{S}_{n,m})_{u,v})] \odot ((\tilde{V}_n)_u)\,|_{(z_u)\,=\,(0)} \\ = ((\tilde{S}_{n,m})_{u,v}) \odot ((\tilde{V}_{s_n})_u)\end{aligned} \tag{A.8}$$

With the abbreviated symbol $((\tilde{V}_n)_u)$ for $((\tilde{V}_n)_u)|_{(z_u)\,=\,(0)}$, this equation is duplicated as Equation 2.1 of Section II.

APPENDIX B

TRANSMISSION COEFFICIENTS (MATRIX) FOR APERTURE PENETRATION

To quantify the wire-to-wire interaction through an aperture, the source quantities one needs to know are the voltage and current on the wire in the outer layer. To define the transmission coefficients for such an interaction mechanism, appropriate source reference quantities constructed from this voltage and current have to be used. In Section II, the transmission coefficients have been defined using only the combined voltage

$$\tilde{V}^{(+)}_{\alpha;\lambda} + \tilde{Z}_{c_{\alpha;\lambda}} \tilde{I}^{(+)}_{\alpha;\lambda}$$

of the incoming wave (with respect to the point where the wire penetrates or is attached to the shield, see Figure 2.3a) on the wire in the outer layer as the reference quantity. In this appendix, alternative reference quantities will be used for the definition.

Consider Figure B.1a, where the internal wire is extended in both directions away from the aperture with arbitrary loads. This is a more general configuration than that of Figure 2.3 a. The equivalent circuit for the internal wire of Figure B.1a is given in Figure B.1b. An alternative transmission matrix using the combined voltages of both waves as reference quantities will now be defined. The transmission matrix is given via

$$\begin{pmatrix} \tilde{V}^{(+)}_{1;2} + \tilde{Z}_{c_2} \tilde{I}^{(+)}_{1;2} \\ \tilde{V}^{(+)}_{2;2} + \tilde{Z}_{c_2} \tilde{I}^{(+)}_{2;2} \end{pmatrix} = \begin{pmatrix} \tilde{T}_{1,1;2,1} & \tilde{T}_{1,2;2,1} \\ \tilde{T}_{2,1;2,1} & \tilde{T}_{2,2;2,1} \end{pmatrix} \cdot \begin{pmatrix} \tilde{V}^{(+)}_{1;1} + \tilde{Z}_{c_1} \tilde{I}^{(+)}_{1;1} \\ \tilde{V}^{(+)}_{1;1} - \tilde{Z}_{c_1} \tilde{I}^{(+)}_{1;1} \end{pmatrix}$$
$$+ \begin{pmatrix} \tilde{R}_{1,1;2,2} & 0 \\ 0 & \tilde{R}_{2,2;2,2} \end{pmatrix} \cdot \begin{pmatrix} \tilde{V}^{(+)}_{1;2} - \tilde{Z}_{c_2} \tilde{I}^{(+)}_{1;2} \\ \tilde{V}^{(+)}_{2;2} - \tilde{Z}_{c_2} \tilde{I}^{(+)}_{2;2} \end{pmatrix} \quad (B.1)$$

Here, instead of $\tilde{S}$, $\tilde{T}$ and $\tilde{R}$ are used to distinguish them from the definition of Section II, and to specifically indicate the transmission and reflection

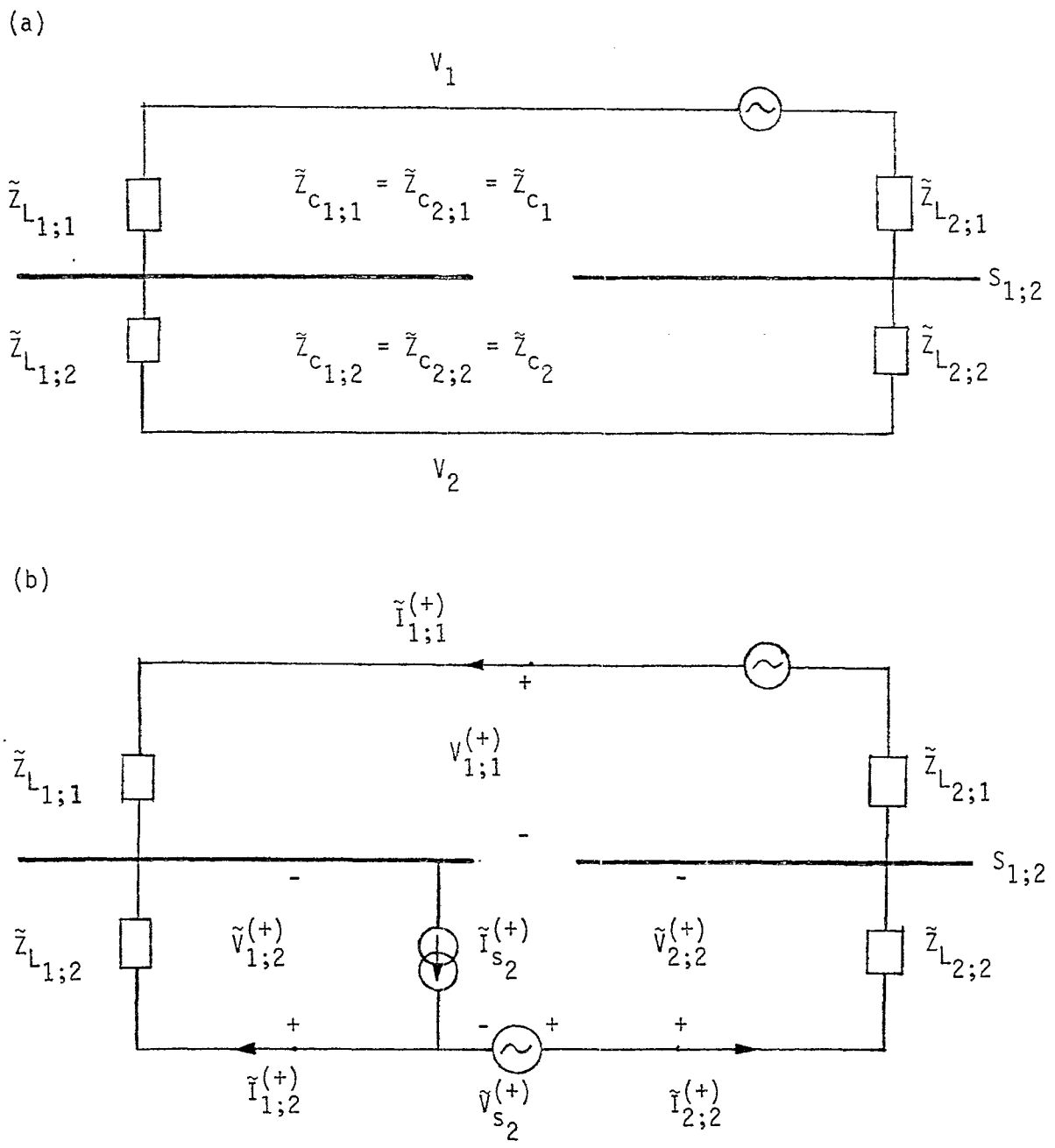

Figure B.1. (a) Schematic drawing of wires interacting through an aperture, and (b) its equivalent circuit for the inner wire.

quantities and $\lambda = 1$, α, $\beta = 1, 2$ are arbitrarily assigned. In order to fit the above definition into the overall scattering matrix formulation, clearly, additional "artificial" wires connecting to the aperture "node" have to be introduced. With Equation B.1, the transmission and reflection coefficients can be calculated. For example, $\tilde{T}_{2,1;2,1}$ can be obtained by solving the circuit of Figure B.1b by taking

$$\tilde{Z}_{L_{2;2}} = \tilde{Z}_{c_2} \quad \text{and} \quad \tilde{Z}_{L_{1;1}} = \tilde{Z}_{c_1}$$

That is, one has,

$$(\tilde{T}) = \begin{pmatrix} \tilde{T}_{1,1;2,1} & \tilde{T}_{1,2;2,1} \\ \tilde{T}_{2,1;2,1} & \tilde{T}_{2,2;2,1} \end{pmatrix}$$

$$= \begin{pmatrix} \dfrac{-\tilde{Z}_{c_2}\,\tilde{v}_{s_{2,1}} + \tilde{Z}_{L_{2;2}}\,\tilde{i}_{s_{2,1}}}{\tilde{Z}_{L_{2;2}} + \tilde{Z}_{c_2}} & \dfrac{\tilde{Z}_{c_2}\,\tilde{v}_{s_{2,1}} + \tilde{Z}_{L_{2;2}}\,\tilde{i}_{s_{2,1}}}{\tilde{Z}_{L_{2;2}} + \tilde{Z}_{c_2}} \\ \dfrac{\tilde{Z}_{c_2}\,\tilde{v}_{s_{2,1}} + \tilde{Z}_{L_{1;2}}\,\tilde{i}_{s_{2,1}}}{\tilde{Z}_{L_{1;2}} + \tilde{Z}_{c_2}} & \dfrac{-\tilde{Z}_{c_2}\,\tilde{v}_{s_{2,1}} + \tilde{Z}_{L_{1;2}}\,\tilde{i}_{s_{2,1}}}{\tilde{Z}_{L_{1;2}} + \tilde{Z}_{c_2}} \end{pmatrix} \qquad \text{(B.2)}$$

and

$$\tilde{R}_{1,1;2,2} = \frac{\tilde{Z}_{L_{2;2}} - \tilde{Z}_{c_2}}{\tilde{Z}_{L_{2;2}} + \tilde{Z}_{c_2}}\,; \quad \tilde{R}_{2,2;2,2} = \frac{\tilde{Z}_{L_{1;2}} - \tilde{Z}_{c_2}}{\tilde{Z}_{L_{1;2}} + \tilde{Z}_{c_2}} \qquad \text{(B.3)}$$

Various natural matrix norms can be calculated for the transmission matrix $(\tilde{T})$. For example,

$$\|(\tilde{T})\|_\infty = \max \left\{ \frac{\left| -\tilde{Z}_{c_2} \tilde{v}_{s_{2,1}} + \tilde{Z}_{L_{j;2}} \tilde{i}_{s_{2,1}} \right| + \left| \tilde{Z}_{c_2} \tilde{v}_{s_{2,1}} + \tilde{Z}_{L_{j;2}} \tilde{i}_{s_{2,1}} \right|}{\left| \tilde{Z}_{L_{j;2}} + \tilde{Z}_{c_2} \right|} ; \; j = 1,2 \right\}$$

$$= \begin{cases} 2 \left| \tilde{i}_{s_{2,1}} \right| , \text{ for } \tilde{Z}_{L_{j;2}} = \infty, \; j=1,2 \\ 2 \left| \tilde{v}_{s_{2,1}} \right| , \text{ for } \tilde{Z}_{L_{j;2}} = 0, \; j = 1,2 \\ \max \left\{ 2 \left| \tilde{v}_{s_{2,1}} \right| ; \; 2 \left| \tilde{i}_{s_{2,1}} \right| \right\}, \text{ for } \tilde{Z}_{L_{1;2}} = 0, \; \tilde{Z}_{L_{2;2}} = \infty \\ \frac{1}{2} \left| \tilde{v}_{s_{2,1}} + \tilde{i}_{s_{2,1}} \right| + \frac{1}{2} \left| -\tilde{v}_{s_{2,1}} + \tilde{i}_{s_{2,1}} \right| < \left| \tilde{v}_{s_{2,1}} \right| + \left| \tilde{i}_{s_{2,1}} \right| \\ \quad \text{(equal when } \tilde{v}_{s_{2,1}} / \tilde{i}_{s_{2,1}} \text{ is real), for } \tilde{Z}_{L_{j;2}} = \tilde{Z}_{c_2} , \; j = 1,2 \end{cases} \quad (B.4)$$

and,

$$\|(\tilde{T})\|_2 = \max \left\{ \left| \frac{2\tilde{Z}_{c_2} \tilde{v}_{s_{2,1}}}{\tilde{Z}_{L_{1;2}} + \tilde{Z}_{c_2}} \right| ; \left| \frac{2\tilde{Z}_{L_{1;2}} \tilde{i}_{s_{2,1}}}{\tilde{Z}_{L_{1;2}} + \tilde{Z}_{c_2}} \right| \right\}, \text{ for } \tilde{Z}_{L_{1;2}} = \tilde{Z}_{L_{2;2}}$$

$$= \begin{cases} 2 \left| \tilde{i}_{s_{2,1}} \right| , \text{ for } \tilde{Z}_{L_{j;2}} = \infty , \; j = 1, \; 2 \\ 2 \left| \tilde{v}_{s_{2,1}} \right| , \text{ for } \tilde{Z}_{L_{j;2}} = 0, \; j = 1, \; 2 \\ \max \left\{ \left| \tilde{v}_{s_{2,1}} \right| ; \; \left| \tilde{i}_{s_{2,1}} \right| \right\}, \text{ for } \tilde{Z}_{L_{j;2}} = \tilde{Z}_{c_2} , \; j = 1, \; 2 \end{cases} \quad (B.5)$$

The above consideration, of course, can be used for the wire-to-wire aperture penetration configuration discussed in Subsection II.3.a, i.e., Figure 2.3. For that configuration (taking $\lambda = 1$, $\beta = 2$, $\alpha = 1$), Equation B.1 reduces to

$$\tilde{V}^{(+)}_{2;2} + \tilde{Z}_{c_2}\,\tilde{I}^{(+)}_{2;2} = \tilde{T}_{2,1;2,1}\,[\tilde{V}^{(+)}_{1,1} + \tilde{Z}_{c_1}\,\tilde{I}^{(+)}_{1;1}] + \tilde{T}_{2,2;2,1}\,[\tilde{V}^{(+)}_{1;1} - \tilde{Z}_{c_1}\,\tilde{I}^{(+)}_{1;1}] \tag{B.6}$$

Then, one has, in the norm (magnitude, for a scalar) sense,

$$\begin{aligned}
\left|\tilde{V}^{(+)}_{2;2} + \tilde{Z}_{c_2}\,\tilde{I}^{(+)}_{2;2}\right| &\le \left|\tilde{T}_{2,1;2,1}\right| \left|\tilde{V}^{(+)}_{1;1} + \tilde{Z}_{c_1}\,\tilde{I}^{(+)}_{1;1}\right| \\
&\quad + \left|\tilde{T}_{2,2;2,1}\right| \left|\tilde{V}^{(+)}_{1;1} - \tilde{Z}_{c_1}\,\tilde{I}^{(+)}_{1;1}\right| \\
&\le \left\{\left|\tilde{T}_{2,1;2,1}\right| + \left|\tilde{T}_{2,2;2,1}\right|\right\} \left|\tilde{V}^{(+)}_{1;1} + \tilde{Z}_{c_1}\,\tilde{I}^{(+)}_{1;1}\right| \\
&\qquad \text{if } \left|\tilde{V}^{(+)}_{1;1} + \tilde{Z}_{c_1}\,\tilde{I}^{(+)}_{1;1}\right| \ge \left|\tilde{V}^{(+)}_{1;1} - \tilde{Z}_{c_1}\,\tilde{I}^{(+)}_{1;1}\right| \\
&\le \max\left\{2\left|\tilde{v}_{s_{2,1}}\right|; 2\left|\tilde{i}_{s_{2,1}}\right|\right\} \left|\tilde{V}_{1;1} + \tilde{Z}_{c_1}\,\tilde{I}^{(+)}_{1;1}\right|
\end{aligned} \tag{B.7}$$

which agrees with Equation 2.10 where a transmission coefficient was defined using only

$$\tilde{V}^{(+)}_{1;1} + \tilde{Z}_{c_1}\,\tilde{I}_{1;1}$$

as the reference source quantity.

So far, the discussion in this appendix deals with the wire-to-wire aperture penetration problem. The same procedure can be used for the field-to-wire aperture penetration problem so that, instead of just $a\left[\tilde{E}_{sc} + Z_o\tilde{H}_{sc}\right]$, both $a\left[\tilde{E}_{sc} \pm Z_o\tilde{H}_{sc}\right]$ can be used for the transmission matrix definition. That is, similar to Equation B.1, one has

$$\begin{pmatrix} \tilde{V}^{(+)}_{1;2} + \tilde{Z}_{c_2}\,\tilde{I}^{(+)}_{1;2} \\ \tilde{V}^{(+)}_{2;2} + \tilde{Z}_{c_2}\,\tilde{I}^{(+)}_{2;2} \end{pmatrix} = \begin{pmatrix} \tilde{T}_{1,1;2,1} & \tilde{T}_{1,2;2,1} \\ \tilde{T}_{2,1;2,1} & \tilde{T}_{2,2;2,1} \end{pmatrix} \cdot \begin{pmatrix} a\left[\tilde{E}_{sc} + Z_o\tilde{H}_{sc}\right] \\ a\left[\tilde{E}_{sc} - Z_o\tilde{H}_{sc}\right] \end{pmatrix}$$

$$+ \begin{pmatrix} \tilde{R}_{1,1;2,2} & 0 \\ 0 & \tilde{R}_{2,2;2,2} \end{pmatrix} \cdot \begin{pmatrix} \tilde{V}^{(+)}_{1;2} - \tilde{Z}_{c_2}\,\tilde{I}^{(+)}_{1;2} \\ \tilde{V}^{(+)}_{2;2} - \tilde{Z}_{c_2}\,\tilde{I}^{(+)}_{2;2} \end{pmatrix} \quad \text{(B.8)}$$

With Equation B.8, one can proceed as before to obtain relations the same as Equations B.2 through B.7, except that $\tilde{v}_{s_{2,1}}$ and $\tilde{i}_{s_{2,1}}$ have to be changed to $\tilde{v}^{(f)}_{s_{2,1}}$ and $\tilde{i}^{(f)}_{s_{2,1}}$.

GLOSSARY

Indices (appeared as subscripts)

u or v	wave index
λ or η	layer (volume) index
ℓ or ℓ'	sublayer index
τ or τ'	elementary layer index
μ or μ'	layer-part index (= 1, 2, 3)
σ or σ'	dual-wave index (= 1, 2)
n or m	wire (POE) index

$\mu \rightarrow (\alpha;\lambda) \rightarrow (\sigma;\tau;\ell;\mu;\lambda)$

Superscripts

(+)	for true quantities (to be in contrast with combined quantities)
(L)	for "line" penetrations
(f)	for "field" aperture penetrations
(i)	aperture index

General matrix/vector symbols

$( )$	matrix/vector symbol
$\odot$	generalized dot product
$\cdot$	dot product
$((\tilde{A}_{n,m})_{u,v})$	supermatrix whose element $\tilde{A}_{n,m;u,v}$ is associated with n-wire of u-wave and m-wire of v-wave
$((\tilde{B}_{n})_{u})$	supervector whose element $\tilde{B}_{n;u}$ is associated with n-wire of u-wave
$((1_{n,m})_{u,v})$	identity supermatrix
$((0_{n,m})_{u,v})$	zero supermatrix
$( )^{-1}$	inverse of a matrix

$( )^{\dagger}$	conjugate transpose of a matrix
$\rho\{( )\}$	spectral radius of a matrix
$\|( )\|$	natural matrix/vector norm
$\|( )\|_p$	p-norm, p=1,2,...., ∞

Symbols associated with EM topology and interaction

$V_{\lambda,\ell}$	ℓ-sublayer in λ-layer
$S_{\lambda,\ell;\lambda+1,\ell'}$	surface separating ℓ-sublayer in λ-layer from ℓ'-sublayer in $(\lambda+1)$ - layer
W_u	u-wave
$\tilde{V}_{n;u}$	combined voltage on n-wire of u-wave
$\tilde{V}^{(+)}_{n;u}$, $\tilde{I}^{(+)}_{n;u}$	true voltage, current on n-wire of u-wave
$\tilde{V}_{s_{n;u}}$	combined source voltage on n-wire of u-wave
$\tilde{V}^{(+)}_{s_{n;u}}$, $\tilde{I}^{(+)}_{s_{n;u}}$	true source voltage, source current on n-wire of u-wave
$\tilde{S}_{n,m;u,v}$	scattering coefficient which scatters combined voltage on m-wire of v-wave into n-wire of u-wave
$\tilde{I}_{n,m;u,v}$	interaction supermatrix element = $1 - \tilde{S}_{n,m;u;v}$
$\tilde{E}_{n;u}$	excitation supervector element, with $((\tilde{E})_n)_u = ((\tilde{S}_{n,m})_{u,v}) \odot ((\tilde{V}_{s_n})_u)$
$(\tilde{Z}_{c_{n,m}})_{u,v} = 1_{u,v}(\tilde{Z}_{c_{n,m}})_u$	normalization impedance matrix for wires on an edge containing u- and v-wave; $1_{u,v}$ = Kronecker delta function, =1 for u=v, =0 for u≠v.
a	normalization length used in field-to-wire aperture interaction
$\tilde{I}^{(+)}_{s_{\lambda+1}}$, $\tilde{V}^{(+)}_{s_{\lambda+1}}$ [$\tilde{I}^{(f)}_{s_{\lambda+1}}$, $\tilde{V}^{(f)}_{s_{\lambda+1}}$]	true equivalent current source, voltage source on a wire in $(\lambda+1)$ - layer due to wire-to-wire [field-to-wire] aperture interaction, superscripts "+" have been neglected for simplicity for the field-to-wire interaction

$\begin{cases} \tilde{i}_{s_{\lambda+1,\lambda}}, \tilde{v}_{s_{\lambda+1,\lambda}} \\ [\tilde{i}^{(f)}_{s_{\lambda+1,\lambda}}, \tilde{v}^{(f)}_{s_{\lambda+1,\lambda}}] \end{cases}$	normalized equivalent current source, voltage source on a wire in $(\lambda+1)$ - layer due to interaction through an aperture from wire [field] in λ-layer, see Figures 2.3, 2.4 for definition
$\begin{cases} \tilde{\Phi}_m, \tilde{\Phi}_e \\ [\tilde{\Phi}^{(f)}_m, \tilde{\Phi}^{(f)}_e] \end{cases}$	magnetic flux linkage, electric charge deposited on wire due to wire-to-wire [field-to-wire] aperture interaction
α_m, α_e	magnetic, electric polarizability
$\tilde{E}_{sc}, \tilde{H}_{sc}, \tilde{\sigma}_{sc}, \tilde{J}_{sc}$	short-circuited electric field, magnetic field, surface charge density, surface current density
$\tilde{V}_{oc}, \tilde{I}_{sc}$	open-circuited voltage, short-circuited current
$\tilde{Z}_{in}, \tilde{Z}_L$	input impedance, loading impedance
R	radius of exclusion region or volume
r_o	wire radius
A	effective aperture area
A_m	magnetic flux penetration factor = $\tilde{\Phi}_m/(\mu_o \tilde{H}_{sc})$